

INDEX

Introduction	3
1. Literature	4
1.1 Additive Manufacturing.....	5
1.1.1 Avio Aero-a GE Aviation Business & Additive Manufacturing.....	5
1.1.2 DMLM Process.....	7
1.1.3 DMLM Point of attention	8
1.2 Optimization	13
1.2.1 Optimization Methods.....	13
1.3 Optimization techniques	15
1.3.1 Concept Design.....	15
1.3.2 Design Fine-Tuning	25
2. Aim of the activity	36
3. Design for Additive guidelines	38
3.1 Problem Definition	38
3.2 Design Optimization	38
3.3 Design Validation.....	40
4. Exercise of Topology optimization with Overhang constraint.....	41
5. Exercise of Optimization on Dummy Conical Housing	43
5.1 Problem Definition	43
5.2 Design Optimization	46
5.2.1 Free-Size static-dynamic 2D	48
5.2.2 Topography static-dynamic 2D.....	48
5.2.3 Topology static-dynamic 3D	49
5.2.4 Conclusion of Conceptual Design	50
6. Exercise of Optimization of a Turboprop Engine Housing	51
6.1 Problem Definition	51

6.1.1 Introduction to Engine.....	51
6.1.2 Baseline.....	54
6.2 Design Optimization	58
6.3.1 Free-Size on Shell Design	60
6.3.2 Topography on Shell Design	61
6.3.3 Topology on Design Space 3D	62
6.3.4 Conclusion of Conceptual Design	64
6.3 Design Validation	67
Conclusions	68
Bibliography.....	69

A new mission statement of the design engineer becomes reality: What is thinkable is designable, and what is designable is manufacturable.

Introduction

Proven to be effective in creating light-weight, durable and complex aerospace parts, Additive Manufacturing (AM) has been at the forefront of aerospace companies' technology adoption. The commercial aviation industry has high performance standards to comply with and has now accepted AM in the manufacturing of parts such as panel covers, heat exchangers, air conditioning ducts, some interior parts as well as lots of mounting and attachment hardware. This new process requires a new approach to design considering the related issues. Unfortunately, it is impossible at the state of the art deeming all of them.

Moreover, the computer aided structural optimization has gained a lot of potentiality thanks to additive capability to produce complex shape. According to [12], optimizations could be divided in Conceptual and Design Fine-Tuning. Consequently, examples of both types of optimizations have been explored during this thesis project in order to understand properly each behaviour.

Different workflows for design for AM are available in the literature. Relying on these, in this thesis a new methodology for Design Optimization phase has been defined. Certainly, proposed guidelines may change in future, especially when software will be able to handle a great number of variables combining both design phase and processing phase.

The aim of the activity has been to achieve know-how about potentiality of each type of optimization to choose which of them was more suitable to apply to a real test case study keeping in mind the possible constraints associated to AM process. It will be explained that the optimization is not a linear process but is formed by a series of loops where feedback is important.

Lastly, mathematical models of many real-world systems are rather complex and may include a large number of degrees of freedom. In order to handle these models, reduction techniques are available, reducing the size of the model without losing important information on the behaviour of the system. Therefore, one component has been reduced and considered during simulations to show how reduction can work.

1. Literature

This chapter is an introductory section reporting some basic arguments useful for the work thesis. It is structured in three parts, where the first one concerns development and application of additive manufacturing, the second part concerns definition of optimization problem and the last one is an overview of available optimizations techniques for the work thesis.

The first part is a brief summary about application of Additive Manufacturing by GE and by Avio Aero a-GE Aviation Business. The Selective Laser Melting has become a manufacturing method widely used by several industries such as automotive and aerospace [1]. In literature there are a lot of examples of guidelines of design for Additive Manufacturing using Direct Metal Laser Melting (DMLM). For these reasons, DMLM and issue related to this technology have been investigated.

In the second part a definition of optimization process, a classification and fields application fields are presented. A brief overview on three investigation methods of the minima for function of several variables is done. Steps of an iterative procedure known as the local approximation method to determine the solution of the optimization problem are reported.

The third part is a detailed explanation of optimization techniques available for the study of optimization of real test case. Each optimization technique presented has been implemented in a way to better understand strengths and weaknesses depending on case study. At least an example for each optimization technique has been reported.

1.1 Additive Manufacturing

Since even more complex geometries at restrained costs are required, Additive Manufacturing (AM) is a technology object of continuous investigation and development. It was born in 1980s as rapid prototyping. The aerospace industry has incorporated AM throughout its product development lifecycle; from the design concept to repairs. With the various advantages that AM technologies promise, aerospace continues to discover and find new applications and invest in research to make them possible [2]. The Selective Laser Melting has become a manufacturing method widely used by several industries such as automotive and aerospace and has enabled production of parts with geometries which would be impossible to produce with traditional fabrication.

1.1.1 Avio Aero-a GE Aviation Business & Additive Manufacturing

Avio Aero is a GE Aviation business that designs, manufactures and maintains components and systems for civil and military aviation. Provide their customers with innovative technology solutions to quickly respond to the endless changes required by the market: additive manufacturing, rapid prototyping, as well as technologies dedicated to the production of mechanical transmissions, turbines and combustors. Italy is home to the main headquarters and important plants in Turin, Pomigliano d'Arco (Naples) and Brindisi. In 2013 Avio Aero launched in Cameri (Novara) one of the largest plants in the world designed specifically for additive manufacturing. The Turin Additive Laboratory started to operate in 2017 hosting machines which use 3D metal printing technology to combine virtual and experimental HW experience for innovation. Avio Aero and Turin Polytechnic decided to open this new research center dedicated to additive manufacturing in order to exploit the business's industrial and engineering competencies, combining them with the University's expertise in materials and additive technologies research [30,31,32].

Additive manufacturing has helped the GE team to bring the new Turboprop engine from an idea to a working machine in record time. The project was announced on 2015 and on 2017 GE Aviation announced first run of the considered engine. The new 1,240 SHP-rated is the first turboprop engine in its class to introduce two stages of variable stator vanes and cooled high-pressure turbine blades [33,34].

The new Turboprop engine includes more printed components than any production engine in aviation history with 35 percent of the turboprop's parts built via additive manufacturing. A total of 855 conventionally manufactured parts has been reduced to 12 additive parts, including sumps,

bearing housings, frames, exhaust case, combustor liner, heat exchangers and stationary flow path components. Additive components reduce the weight of the engine by 5 percent while contributing a 1 percent improvement in specific fuel consumption.

The main Avio Aero responsibilities are Engine Systems, Control System and Software, Combustion System and both the Power and Accessory gearboxes. Power gearbox is the first Avio Aero gearbox featuring an Additive Main Housing. The combustor has been designed by the Avio Aero engineers around a “reverse flow” configuration to minimize its length and to improve overall engine weight and installation. In this case too additive has been proven to be a real game changer. In addition to the flexibility introduced in the mechanical and thermal design, additive gave the possibility to prototype and test several design concepts which conventional manufacturing processes would not allow within the program schedule.

The engine will power Textron Aviation’s new Cessna Denali, which is expected to fly in late 2018. Full production is expected to begin in 2020. It will eventually provide the thrust for Cessna’s new single-engine, 10-person business aircraft design called Denali fig. 1.



Figure 1: The new Turboprop engine will power Cessna’s new single-engine, 10-person business aircraft design called Denali. Image credit: Textron Aviation [33].

1.1.2 DMLM Process

Manufacturing systems could be divided into three categories for metal applications: powder bed systems, powder feed systems and wire feed systems. Here only powder bed process is presented because from literature this results the most relevant process to realize metal products.

Nowadays the most advanced processes of this category are Electron Beam Melting (EBM), Selective Laser Sintering (SLS) and Selective Laser Melting (SLM), otherwise for metal we can refer as Direct Metal Laser Sintering (DMLS) or Direct Metal Laser Melting (DMLM). Currently with these technologies metals like Inconel, stainless steel, tool steel, titanium, cobalt chrome and aluminium can be used. SLS is an AM method where the metal powder gets partially melted layer-by-layer with a laser. The SLM method is developed to obtain a material denser (up to 99,9%) using a complete melting [29]. In this way inclusions and pores are reduced, which result a problem on the mechanical properties.

The majority of the research conducted by companies, that are developing components with metal powder bed fusion process, are focused on SLM because it is one of the most promising and flexible processes [3]. The basic concept of SLM process is that a moving laser beam is used to melt selectively powdered metal into successive cross-sections of a three-dimensional part. Parts are manufactured on a mobile table moving downward by steps equal to the thickness of the layer. The first process step consists of deposition of the powder layer and the second one of selective melting of the areas to be built-up. These steps are reiterated until the part has been completely built-up. A simple scheme and an image of process are reported in fig. 2.

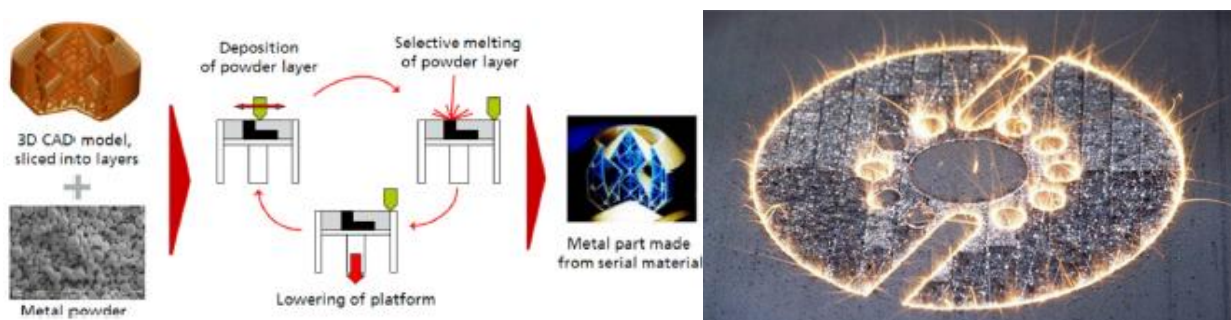


Figure 2 Left: Scheme of SLM; Right: Process image of SLM [3]

The entire operation is run in a protective gas environment (N_2 , Ar) during the described procedures to prevent unwanted reactions and oxidations. Because of the powdered material is “free of binding and fluxing agents” and because it is “heated to its melting temperature throughout the layer

thickness”, the resulting solid has mechanical properties similar to bulk-formed materials. As each layer is selectively melted in this way, the build table in the printer drops down the distance of one-layer thickness (20–100 μm), and a wiper deposits a fresh layer of new un-melted powder, starting the whole operation over again. This cycle continues until the part is complete [4].

1.1.3 DMLM Point of attention

In this section most of information have been taken in a review called “Overhanging Features and the SLM/DMLS Residual Stresses Problem” of Albert E. Patterson et Al. [4]. SLM compared to other metal-melting AM processes is very cost effective; works well with a wide variety of elemental metals and alloys, produces an excellent surface finish, provides excellent feature resolution and is more industrially safe. Unfortunately, the SLM process is known to introduce large amounts of residual stress, due to the large thermal gradients which are inherently present in the process because of the interaction between the laser and the powder. Due to high heating and cooling rates associated with cycling, important plastic strain develops and therefore the thermal gradient (fig. 3) [5]. It can be a major problem because this can initiate cracks, warpage and delamination if the part is not properly designed or has delicate features, both during and after processing, and can reduce the fatigue strength of the part by a factor of 10 or more when compared to bulk-formed parts.

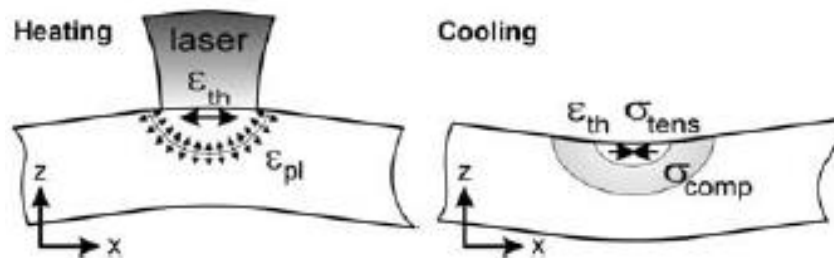


Figure 3 stress gradients in single layers [5]

These problems are especially apparent and challenging in parts with overhanging or protruding features, as the stresses tend to build up more seriously in and near these features during printing; this can cause severe warping and damage to the features and cause the destruction of the entire part, sometimes before it is even finished printing. Temporary support structures, introducing its own problems, can be used to prevent in-process failure.

There are several ways to combat the residual stresses problem when printing very simple parts; most parts created by SLM are physically connected to the build plate at the base, helping to both

support and tie down the layers until the part body is large enough to support the stresses. This is accomplished by fusing the first layer of powder directly to the build plate as if it were the material substrate. Unfortunately, there is not a solid experimentally-based information to be found concerning the effects of the residual stresses on the design of complex parts with overhanging or protruding features (fig. 4). Most of the studies typically discussed in literature searches discuss rule-of-thumb ways to physically prevent the stresses from destroying the parts during printing and trying to understand how the stress directly affect the overhanging features.

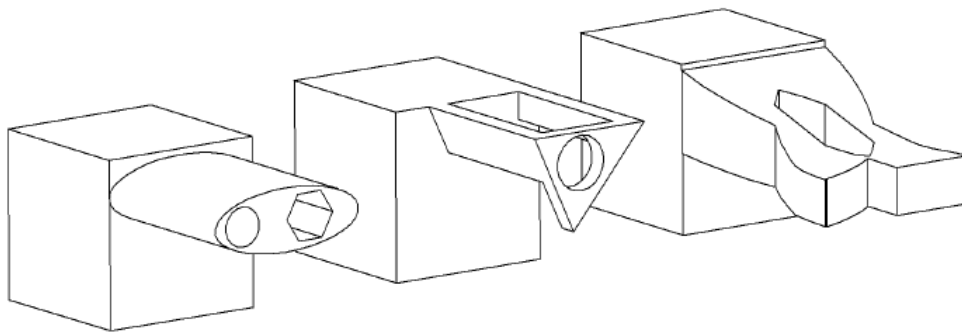


Figure 4 Examples of overhanging and protruding part features [4]

Up to now, the best solution has been to use strong support materials, in spite of some problems using both a powder bed and supports; concerns included the required extra post-processing, extra material use, increased cycle time, increased risk of damage to the part, damage to the finish of the part from support removal and restrictions on the part design to accommodate the support structure; all are issues when using support structures with SLM. Data from several studies suggested that the use of rigid support structures during SLM/SLS for overhanging features may actually cause the residual stresses to be worse than if the overhang had no solid support during printing. To identify a method to combat negative effects residual stresses within overhanging and protruding features, the reviews [4] explores previous work on the topic in-depth in order to define the problem and discover the kind of solutions that may be available to deal with it (fig. 5).

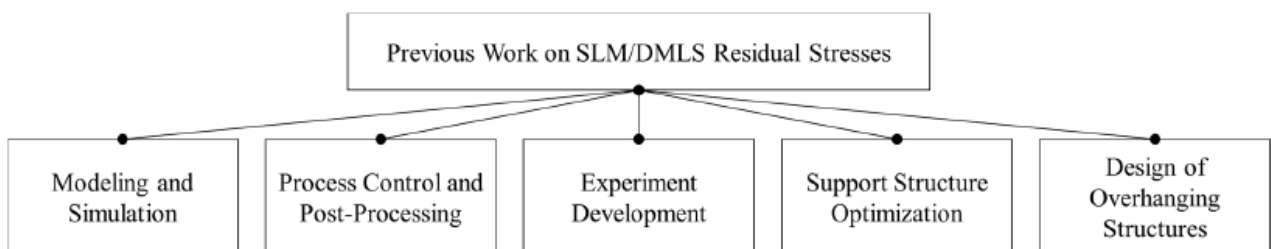


Figure 5 Scheme of areas linked to researches developed on Residual Stresses [4]

As regards “Modeling and Simulation” can be sorted into several subcategories as:

- General SLM process model;
- Temperature distribution and heat transfer models;
- Stress and distortion models;
- Material and microstructure models;

Direct “Process Control and Post-Processing” are the most common and preferred methods of dealing with the residual stresses in practice. Several categories of solutions have been developed:

- Process input control;
- Environment control;
- In Situ monitoring and feedback control;
- Process parameter optimization and post processing;

Experiment methods that have been developed or adapted for use with SLM/SLS can be categorized in:

- Final part testing and Evaluation;
- Optical Process monitoring;
- Mechanical Process monitoring;
- X-Ray and Internal Imaging;
- Design of Experiments;

It should be noted that optimization of removable support materials and the design of overhanging features are separate topics of study and therefore will be discussed separately.

Structural supports are typically needed in order to prevent the failure of unsupported overhanging features. The extra time required to cut, grind or mill off the support structures, the extra material used (which is wasted), the longer print time, the damage to the surface finish when the structure is removed, the extra time required to design the part to accommodate the structure and the design of the structure itself are some of the irritations that come with using SLM to create parts with overhanging features. Now are reported main considerations by literature:

- Sundar et al. [6] found that printing the part on top of a wire mesh made removal from the build plate easier, facilitated the creation of delicate features and thin walls, reduced the

time needed to cut off the support structure and created a buffer to prevent damage to the part itself from the removal.

- There are studies about use of delicate cellular lattice structures as supports taking the advantages like material savings, easier removal from the part, and some time savings compared to methods using solid support structures. However, this takes extra time to design.

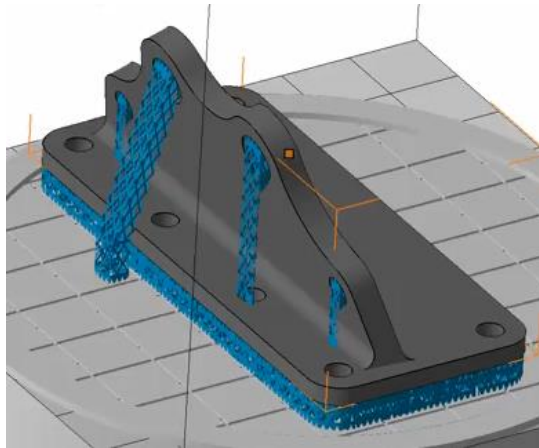


Figure 6 Example of lattice support [7]

Various aspects of **overhanging structures** are now reported:

- Studies focused on the design of curved overhanging parts in a way that not support material or just not significant support material is necessary, have been developed.
- Studies focused on the number of layers needed to provide a stable part overhang with the goal of minimizing the need for the supports altogether. As instance ducts are deeply analysed in literature (fig. 8).

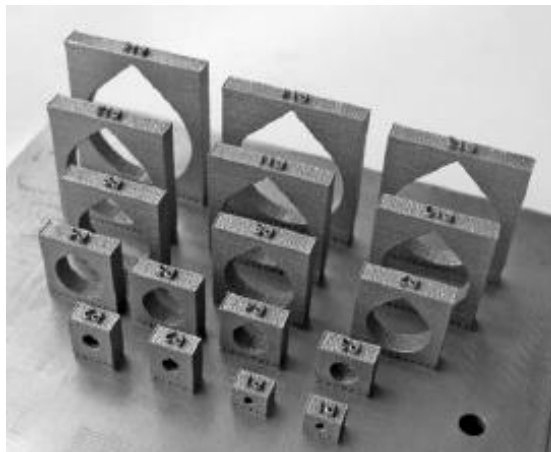


Figure 8 Examples of self-supporting holes designed using specific design rule [8]

- There are studies that defining relationship between process parameters, overhang angle and surface roughness (fig. 9).

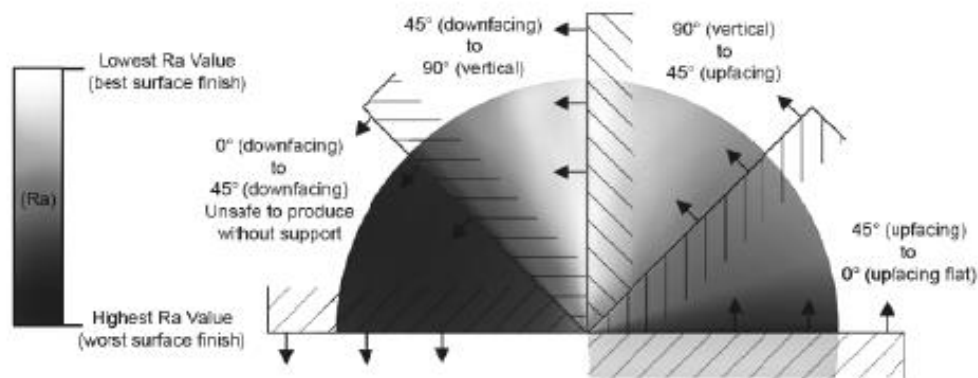


Figure 9 Illustration showing the relationship between orientation and surface quality [8]

- Patterson et al. [41] suggested developing a factorial-based design-of-experiments (DOE) approach to stresses and deformation in 90-degree overhangs, both supported and unsupported. The studies by Patterson et al. were unique because they considered the influence of geometric stress concentrations, as well as the normal part deformation under thermal load. A detailed numerical study and comparison to available experimental data showed that the stress concentration had a very large influence, at least as much as the laser power, on the stress and deformation.

Summarising, nowadays a big effort is moving on careful to produce parts self-supported in a way to avoid waste of material introduced by supports with own issue like post machining. For instance, one of the most famous commercial software includes the manufacturing constraint of overhang in the topology optimization. It permits during design phase to decide grow direction and angle between grow direction and solid parts, the penalization scheme and choice between supported and self-supported building. This constraint is used in some example in this thesis without consider thermal stress. In fig. 10 several experiments with different overhang angles are reported.

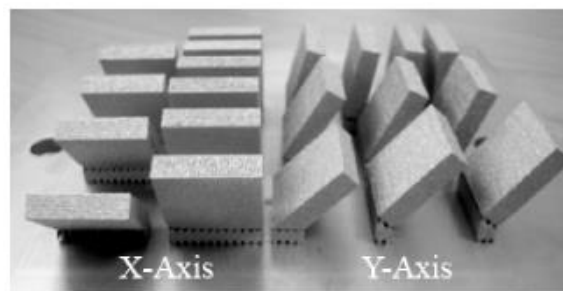


Figure 10 Cuboids built with different overhang angles along X-Axis and Y-Axis [8]

1.2 Optimization

During design process is used investigate principles and procedures of optimization. Optimization process is a mathematical tool governed by an algorithm that changes iteratively design variables, maintaining defined constraint and finding best solution of a problem. It is an instrument applicable in many fields as Structural, Thermal, Acoustic, Fatigue, NVH and Multi-body Dynamics Simulation. Optimization problem could be classified from a mathematical point of view as linear versus nonlinear, static versus dynamic, deterministic versus stochastic, or permanent versus transient. Typical optimization problem is organized as follow:

1. The selection of the vector of design variables x_i that depend on the type of optimization being performed.

$$x_i \text{ with } i = 1, \dots, n ;$$

2. Design Constraints Functions $g_j(x)$ that is response obtained from a finite element analysis. A constraint is considered active if it is satisfied exactly i.e. $g_j(x) = 0$; it is considered inactive if $g_j(x) < 0$; it is considered violated if $g_j(x) > 0$.

$$g_j(x) \leq 0 \text{ with } j = 1, \dots, m;$$

$$\text{and } x_i^L \leq x_i \leq x_i^U \text{ with } i = 1, \dots, n ;$$

3. Objective Function $f(x)$ that is response obtained from a finite element analysis.

$$\min f(x) = f(x_1, x_2, \dots, x_n) ;$$

In this thesis linear structural optimization (static and/or dynamic) is considered. Structural optimization has the aim to improving building in a way that can sustain loads and stresses in a better way. Optimization process seeks to make lighter and stronger by identifying best arrangement of material without violate the stress limit when is it possible.

1.2.1 Optimization Methods

In literature are present a very large amount of optimization methods [29]. It is possible individuate three investigation methods of the minima for function of several variables: Analytic methods based on Gradient (Steepest Descent Method) and Hessian (Newton's Method); Stochastic methods that contain stochastic variables like Simulated Annealing and Genetic Algorithm; Global methods that

allow to gather the greatest number of information about the problem using the lowest amount of resources, e.g. DOE-Design of Experiments.

An iterative procedure known as the local approximation method to determine the solution of the optimization problem use the following steps:

1. Analysis of the physical problem using finite elements method;
2. Convergence test to evaluate if the convergence is achieved or not;
3. Retain potentially active responses for the current iteration;
4. Sensitivity analysis for retained responses;
5. Optimization of problem formulated using the sensitivity information;
6. Back to step 1.

Available software in this thesis utilizes gradient-based optimization algorithms to solve the optimization problem; it has two classes of optimization methods implemented: dual method and primal method. The dual method resolves the optimization problem in the dual space of Lagrange multipliers associated with active constraints. It results very efficient for design problems involving a very large number of design variables but highly fewer constraints and therefore for optimization like Topology or Topography. The primal method checks the optimum in the original design variable space. It is used for problems that involve equally as many design constraints as design variables found in optimization like Size or Shape. Usually the choice of optimizer is made automatically by the software, based on the characteristics of the optimization problem.

When the change in the objective function is less than the objective tolerance and constraint violations are less than 1%, for two consecutive iterations, “regular convergence” is achieved. On the contrary if the constraints remain violated by more than 1%, and for three consecutive iterations the change in the objective function is less than the objective tolerance and the change in the constraint violations is less than 0.2%, design is defined “infeasible” [10].

1.3 Optimization techniques

Preliminary knowledge of the component and its work condition are required because each problem requires different optimization technique. In chapter 6 is shown how available optimizations could be used in sequence to design or redesign a component reaching objectives set demonstrating how the optimization process is not direct but need whatever more optimization phases. Furthermore, there are different kind of optimization depending on the design variables and objective to be achieved. In this chapter a detailed classification of analysed optimizations is presented according to Altair that divide these in optimizations of Concept and of Define Fine-Tuning Design [12]. All the following information have been taken in [10].

1.3.1 Concept Design

Optimizations at the concept level design are techniques to be used in order to define the preliminary geometry of a component. This phase gives the greatest flexibility impacting the design of a product. Employing at this stage the potential for better, more efficient designs, lighter and innovative designs is maximized. The following Topology, Topography and Free-Size optimization for concept design are now explained in detail.

1.3.1.1 Topology

Topology optimization is an automatic process to find the optimal lay-out of a structure within a specified region. This region has to consider design restrictions such as the location and size of prescribed holes or solid areas. Topology optimization has density as design variable inside the Design Space; it is the first technique to be used to define the preliminary loads path and so geometry of a component. This approach is decisive for new components, but also to optimize existing ones. Optimization software generates an optimal design proposal for the most efficient material layout of the design based on user-defined Design Space, design targets and manufacturing process parameters. The following responses are available as objective or as constraint functions:

Mass	Volume	Volume or Mass Fraction
Center of Gravity	Moment of Inertia	Static Compliance
Static Displacement	Natural Frequency	Von Mises Stress on Entire Model (only as constraint)
Buckling Factor (special case)	Frequency Response Displacement, Velocity, Acceleration	Temperature

Weighted Compliance	Weighted Frequency	Combined Compliance Index
Function		

Table 1 Responses for topological optimization in OptiStruct [10]

The following responses are available as the objective or as constraint functions for elements that do not form part of the Design Space:

Static Stress	Static Strain	Static Force
Composite Stress	Composite Strain	Composite Failure Criterion
Frequency Response Stress	Frequency Response Strain	Frequency Response Force

Table 2 Responses for elements that do not form part of the design in topological optimization in OptiStruct [10]

OptiStruct solves Topology optimization problems using the density method, also known as the Solid Isotropic Material with Penalty (SIMP) method in the research community. Under Topology optimization, the material density of each element should take a value of either 0 or 1, defining the element as being either void or solid, respectively. Unfortunately, optimization of a large number of discrete variables is computationally prohibitive, therefore, representation of the material distribution problem in terms of continuous variables has to be used. The material density of each element is directly used as the design variable and varies continuously between 0 and 1. Intermediate values of density represent fictitious material. Techniques need to be introduced to penalize intermediate densities and to force the final design to be represented by densities of 0 or 1 for each element. An interpolation scheme now represented is used to correlate the elastic property with density.

$$E(x) = \rho(x)^p E_0 \quad \text{with } p > 1$$

With

$$E(\rho = 1) = E_0 \quad E(\rho = 0) = 0$$

Where:

- x : is the position vector inside the design domain;
- $\rho(x)$: is the relative density at the position x ;
- $E(x)$: is the material stiffness at the position x ;
- p : is the penalty factor;

The fig. 12 shows correlation between elastic property and density and how penalization factor works.

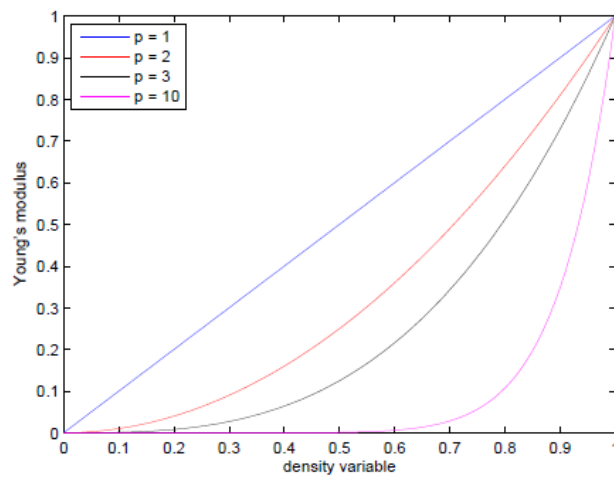


Figure 12: Example of the behaviour of the Young's modulus at different material penalization parameter values using the SIMP method

An example of work flow for this optimization is now presented. The first step is defining Design and Non-Design Space and run Topology optimization (fig. 13).

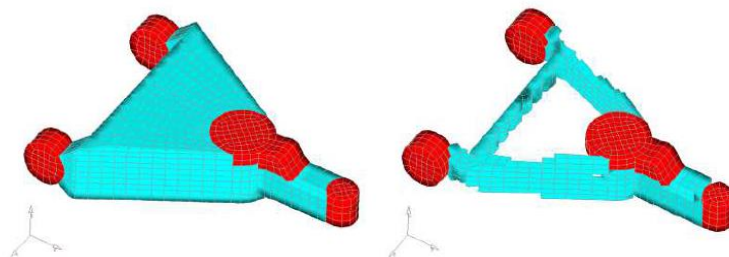


Figure 13 Design and Non-Design definition and Topology optimization results [10]

The second step is interpretate the result reconstructing geometry and performing second loop optimization minimizing the mass while meeting stress and deflection criteria as shown in fig.14.

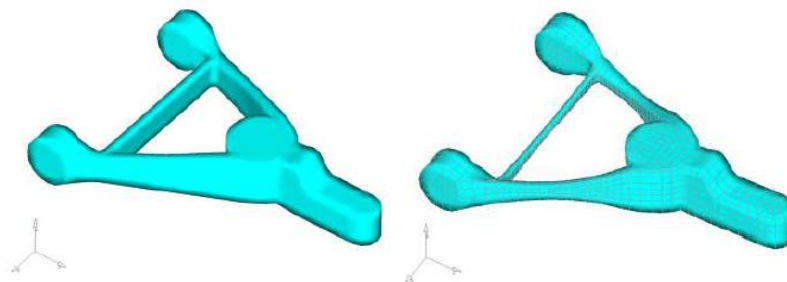


Figure 13.1 Results interpretation and second loop optimization [10]

Second loop optimization will be explained in detail in chapter 6 on test case optimization.

1.3.1.2 Topography

Topography Optimization is used for thin-walled structures or for generate beads or swages to reinforce the structures. For given allowable bead dimensions, Topography optimization technology will generate innovative design proposals with the optimal bead pattern for reinforcement.

Topography optimization is an advanced form of shape optimization in which a design region is defined and a pattern of shape variable-based reinforcements within that region is generated. The design region is subdivided into a large number of separate variables whose influence on the structure is calculated and optimized changing the shape over a series of iterations. Only the shape can be changed, not the thickness. The following responses are currently available as the objective or as constraint functions:

Mass*	Volume*	Center of Gravity
Moment of Inertia	Static Compliance	Static Displacement
Natural Frequency	Buckling Factor	Static Stress, Strain, Forces
Static Composite Stress, Strain, Failure Index	Frequency Response Displacement, Velocity, Acceleration	Frequency Response Stress, Strain, Forces
Weighted Compliance	Weighted Frequency	Combined Compliance Index
Function	Bead discreteness fraction	Temperature
*Mass and Volume are not recommended for use as objectives or constraints since mass and volume are not very sensitive to design changes in topography optimization.		

Table 3 Responses for Topography optimization in OptiStruct [10]

One or more design domains are defined using the DTPG card that must, in turn, reference DESVAR, PSHELL or PCOMP definitions. If a DESVAR is defined, it must be a shape design variable and therefore it must, in turn, be referenced by one or more DVGRID cards. If a PSHELL is defined, shape variables are generated using the parameters defined on the DTPG card, creating internal DVGRID data for the nodes associated with PSHELL definitions. The results in both cases is that each DTPG card references a single shape variable and it is then converted into Topography shape variables.

Basic Topography shape variables follow the parameters defined by the user on DTPG card. The shape is circular and laid out across the design domain in a distribution that is similar to roughly hexagonal shape. The diameter of a circular central region of each topography variable is equal to the Minimum Bead Width. Grids in this region are perturbed as a group. Grids outside of this region

are perturbed as the average of the variables to which they are nearest. If one variable is completely perturbed and its nearby is unperturbed, the nodes in between will form a smooth slope connecting them at an angle equal to the Draw Angle. The spacing of the variables is determined by the minimum bead width and the draw angle in such a way that no part of the bead reinforcement pattern forms an angle greater than the draw angle. Draw Height defines the allowable movement that each node could be reach.

Pattern grouping options allow to obtain shape that you want to obtain according to symmetry or manufacturing constraint. The options are as instance linear, planar, circular, radial and cyclical symmetry controlled in such way the reinforcements follow the desired pattern.

About variable generation there are three methods of automatically generating shape variables for Topography optimization using DTPG card. The first is **element normal**, the second is **draw vector** and third requires that the input data contain one or more shape design variables. We can call the last one as **user defined**.

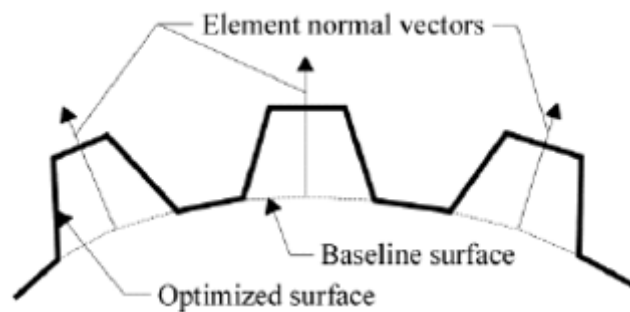


Figure 14 Element normal [10]

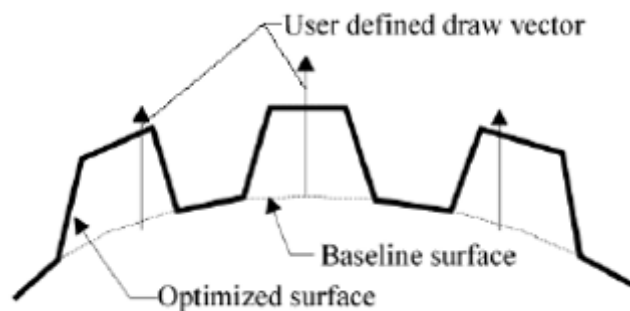


Figure 14.1 Draw vector [10]

To better understand how topography optimization works a simple example of plate in torsion is now reported (fig. 15).

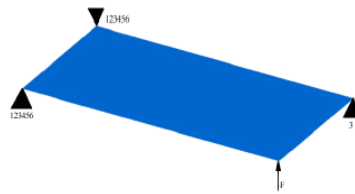


Figure 15 Loads and boundary conditions [10]

The concept explained before about the division of design region into smaller areas, each with its own shape variable could be clearest with the next fig. 15.1.

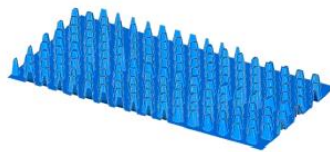


Figure 15.1 Inner portions of the shape variables for the plate [10]

In this optimization the objective is minimise the displacement. The potential reinforcement pattern can be any combination of these variables deflected at any height between zero and the user-defined maximum height. A possible solution for this example is displayed in fig. 15.2.

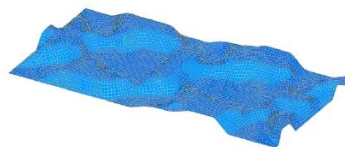


Figure 15.2 Results of optimization [10]

An example of how this optimization can be used in solid model is now reported. It is the case of surface optimization of a control arm. The following control arm model is based on the Topology optimization result as shown in fig. 16.

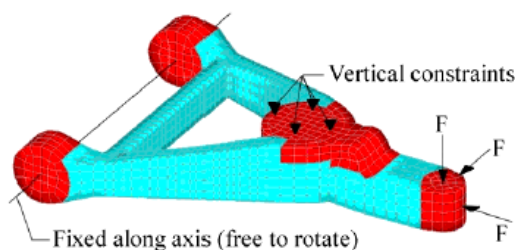


Figure 16 Loads and constraints for solid control arm [10]

After a basic material layout is generated using Topology optimization the solution can be refined to obtain design objectives using shape optimization (meaning: Shape; Topography; Free-Shape). It could be very time-consuming procedure if done by hand with Shape optimization (using HyperMorph), therefore automating the procedure of generating shape variables over the entire surface of a solid part (Topography or Free-Shape) result quickly set up. This consideration will be clear reading section dedicated to Shape optimization. Using Topography optimization to optimize the surface of a solid model, areas to be optimized must previously covered with shell elements as shown in fig. 16.1.

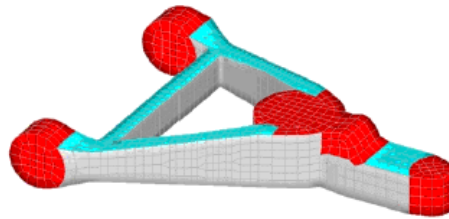


Figure 16.1 Solid control arm model partially covered by grey shell elements [10]

For this example, side surfaces of structural members are optimized. Shells are attached to the sides of the members. The normal vectors of these elements are defined to go inward. Draw Height must be properly chosen so that nodes of solid element in common with shell element are not get turned inside out during the optimization. If this occurs, will be an error and the optimization will be stopped.

The lower bound on the DTPG card is set to -1.0 and the upper bound is set to 1.0 , which allows the control arm to grow or become smaller. The objective is set as minimizing the weighted sum of the compliance of the load cases while holding the mass of the part constant.

The result in fig. 16.2 shows that the rear cross bar is reduced in width; either side of struts the geometry has to be considered like a C-section; the front member is tapered.

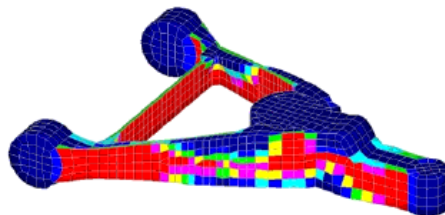


Figure 16.2 Solution for surface optimized control arm, areas to be thinned are red [10]

1.3.1.3 Free-Size

Free-size optimization is largely applied in finding the optimal thickness distribution in machined metallic structures and identifying the optimal ply shapes in laminate composites. Free-Size optimization is an optimization of thickness distribution for shell elements. It allows to understand where most critical areas of structures are and strengthen them. The results are a generation of optimal thickness distributions that meet the design specifications.

Free-size optimization is defined through the DSIZE bulk data entry. Features available for this optimization include: minimum member size control, symmetry, pattern grouping and pattern repetition, and stress constraints applied to Von Mises stresses of the entire structure.

Combine both Topology and Free-Size in the same optimization problem is not recommended by the developers of the software, since penalization on topology components creates a bias that could lead to sub-optimal solutions.

Free-Size optimization allows thickness T to vary freely between T and T_0 for each element.

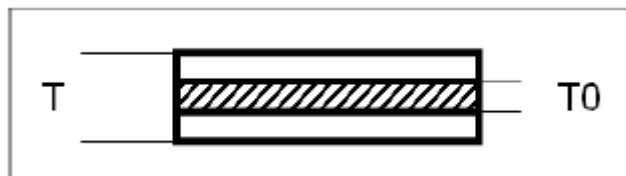


Figure 17 Shell cross-section [10]

In most cases, variable thickness of a shell structure is achieved through step-wise change of thickness. Free-size results provide a different concept about how the zones of different thicknesses should be designed. Detailed Size optimization can then be performed to fine tune the final design. This process is illustrated in the example in fig. 18.

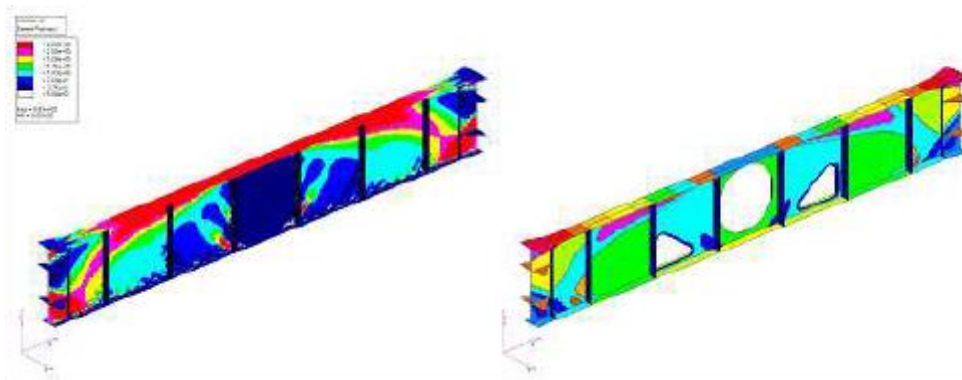


Figure 18 Left: Free-Size result; Right: interpreted zones of constant thickness [10]

In fig. 19 is reported an important example that could be useful to understand that comparing Free-Size optimization on shell element and Topology optimization on solid element with the same depth associated in the property of 2D elements, results are similar.

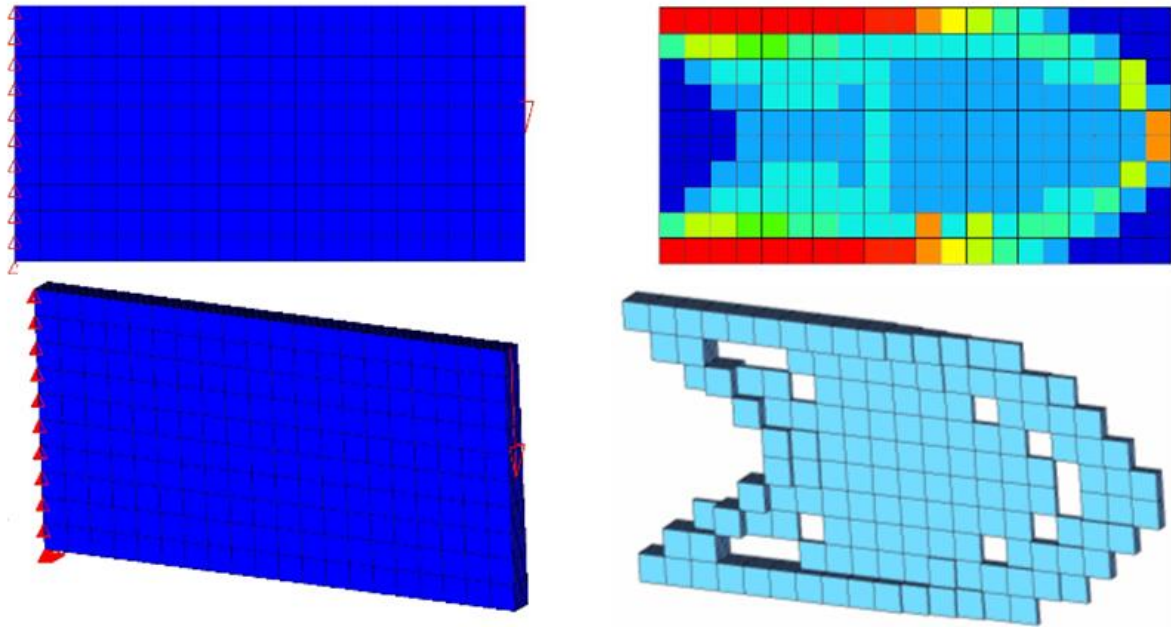


Figure 19 Free-Size and Topology Optimization of Shell Beam [10]

1.3.1.4 Lattice

Singularity to additive manufacturing, is the ability to print lattice structures. Such structures offer many desirable characteristics such as light weight and improved thermal properties. The software has a unique solution to design such lattice structures that is based on Topology optimization but is based on two main phases. Subsequent to the Topology optimization phase, large scale sizing optimization studies can be run on the lattice beams while incorporating detailed performance targets such as stress, buckling, displacement and frequency.

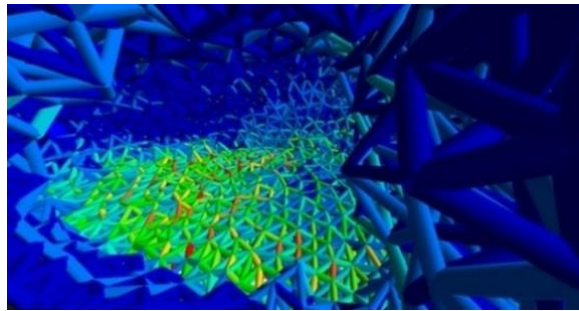


Figure 20 Lattice structure [12]

Lattice Structure Optimization is initially similar to topology optimization; however, design domains can now include elements with intermediate densities. The second phase transforms porous zones from the first phase into explicit lattice structure. Theoretically, from a physical point of view, such structures can be more efficient compared to those in which design elements are penalized to densities of 0 or 1.

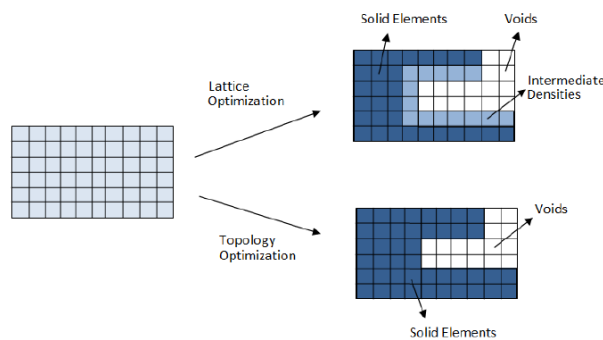


Figure 21 Difference between Lattice optimization (phase 1) and Topology optimization [10]

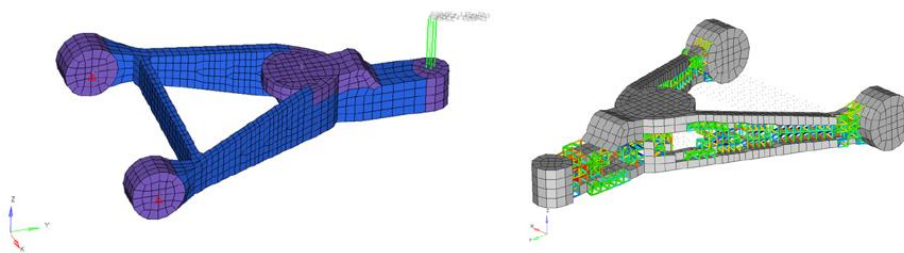


Figure 22 Example of Lattice optimization in OptiStruct (3300) [10]

1.3.2 Design Fine-Tuning

Design Fine-Tuning is used when design changes are limited to changing dimensions (height, length, radii, thicknesses), model parameters (material properties, loads). Parametrization is developed for each problem depending on the parameter type.

1.3.2.1 Size

The software has the capability of performing Size optimization simultaneously with the other types of optimization. In a Size optimization, the properties of structural elements such as shell thickness, beam cross-sectional properties, spring stiffness or mass are modified to solve the optimization problem. Each size variable is defining DESVAR bulk data entry. The following responses in Tab. 4 are currently available as the objective or as constraint functions:

Mass	Volume	Center of Gravity
Moment of Inertia	Static Compliance	Static Displacement
Natural Frequency	Buckling Factor	Static Stress, Strain, Forces
Static Composite Stress, Strain, Failure Index	Frequency Response Displacement, Velocity, Acceleration	Frequency Response Stress, Strain, Forces
Weighted Compliance	Weighted Frequency	Combined Compliance Index
Function	Temperature	

Table 4 Responses for size optimization in OptiStruct [10]

Some structural elements have several parameters depending on each other; like beams in which the area, moments of inertia, and torsional constants depend on the geometry of the cross-section. The property itself is not the design variable in Size optimization, but the property is defined as a function of design variables. The simplest definition, as defined by the design-variable-to-property relationship DVPREL1, is a linear combination of design variables defined on a DESVAR statement such that:

$$p = \sum DV_i \cdot C_i ;$$

Where, p is the property to be optimized, and Ci are linear factors associated to the design variable DV_i. In fig. 23, 23.1, 24 and 25 some examples have been reported.

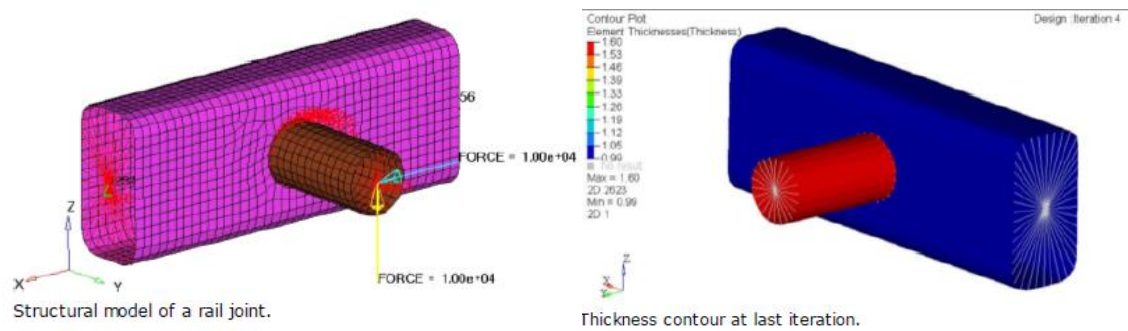


Figure 23 Rail Joint 2D: Minimize volume constraining displacement at loading grid point [10]

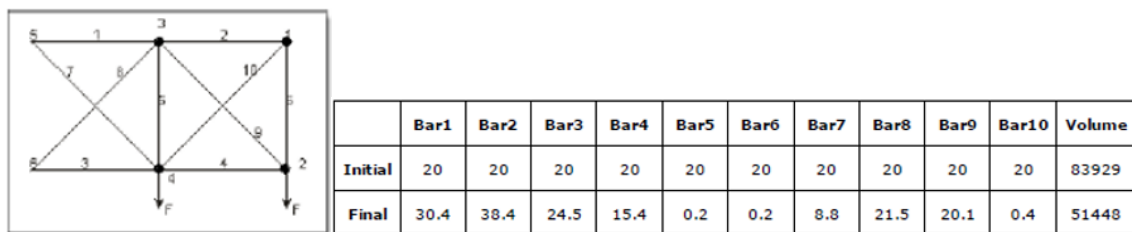


Figure 23.1 Ten bar truss structure 1D: Minimize volume constraining stress

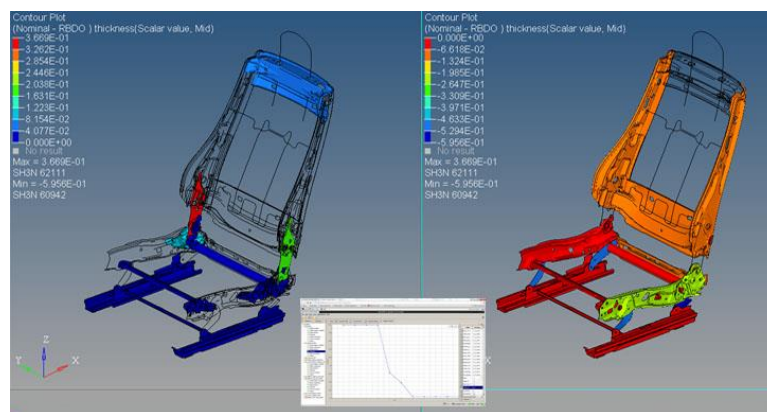


Figure 24 Size Optimization of an Automotive Seat for Safety Load-cases [12]

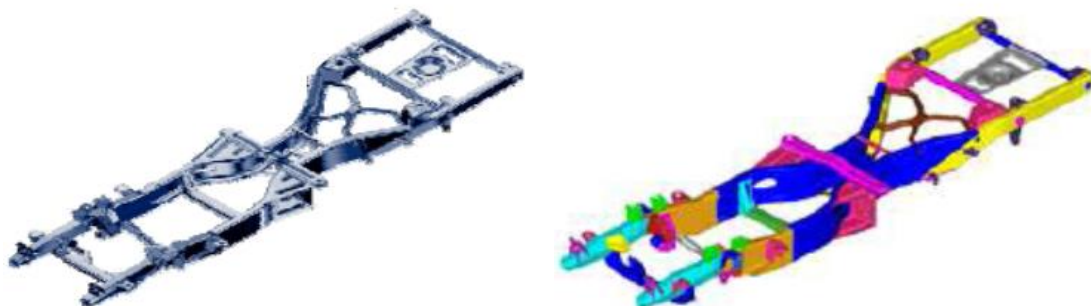


Figure 25 Size Optimization of Thickness Beam of Car Frame [10]

1.3.2.2 Shape

Shape optimization is used to refine an existing design through the shape variables created using HyperMesh's morphing technology, HyperMorph. These shapes variables could be then used by OptiStruct or HyperStudy to update and optimize the design. The outer boundary of the structure is modified to solve the optimization problem. The shape is defined by the grid point locations. Hence, shape modifications change those locations, each shape variable is defined by including DESVAR as bulk data. DVGRID bulk data entries define how much a particular grid point location is changed by the design variable. Any number of DVGRID bulk data entries can be added to the model. Each DVGRID bulk data entry must reference an existing DESVAR bulk data entry if it is to be a part of the optimization. The DVGRID data in OptiStruct contains grid location perturbations. The generation of the design variables and of the DVGRID bulk data entries is facilitated by the HyperMorph utility. The responses available as the objective or as constraint functions are the same of Size optimization. In following images are reported some examples.

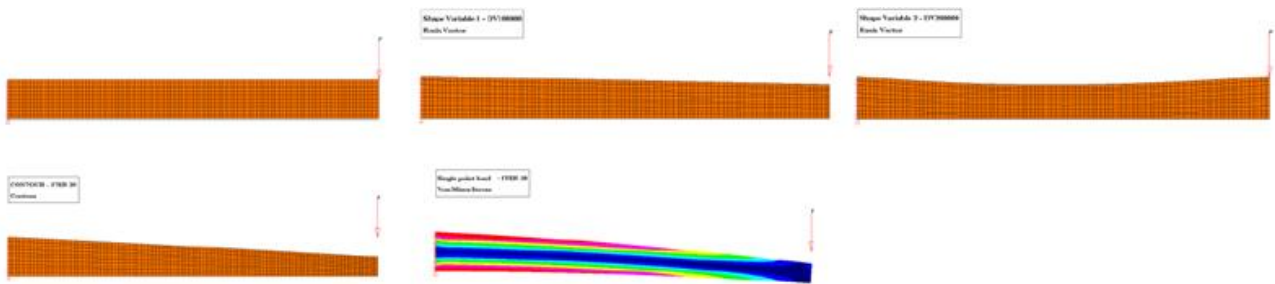


Figure 26 Cantilever Beam 2D: Minimize volume constraining displacement [10]

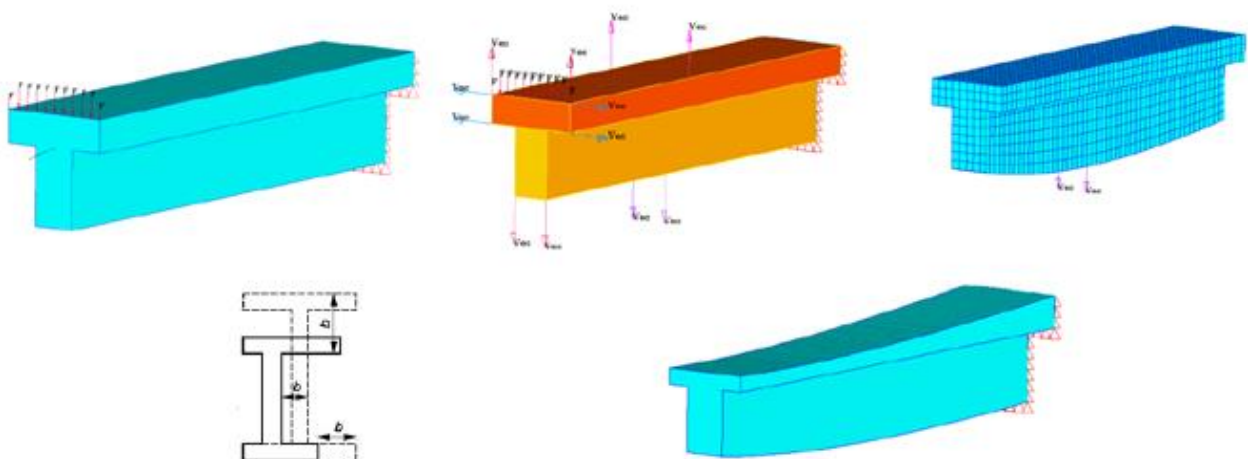


Figure 27 Optimization on Cantilever T Beam 3D [10]

Topography optimization has applications beyond creating beads in shell surfaces. Since the basic topography approach can be applied to any model containing large fields of shape variables, it makes itself suitable to solid model applications.

The following example demonstrates how Topography can be used in conjunction with user-defined shape variables to reach global Shape optimization of a solid part. A solid control arm model is built based around OptiStruct Topology optimization results (see fig. 28). Topology optimization is very effective generating a basic material layout, but the solution is generally not well refined. Refining the solution to meet design requirements can be done using Shape optimization.

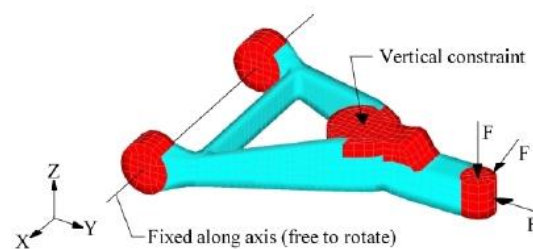


Figure 28 Loads and constraints for solid control arm [10]

The first step is to generate shape variables for the part. For this model, four basic shape variables were created which control the sizes of the two legs and rear beam of the control arm. These are shown below in fig. 28.1 and in fig. 28.2.

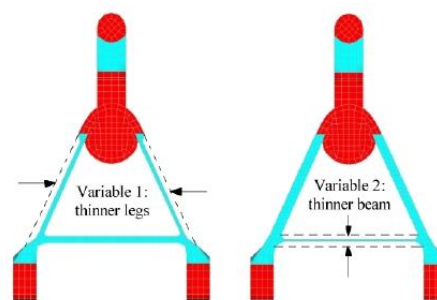


Figure 28.1 Shape variables controlling the thickness of the control arm legs [10]

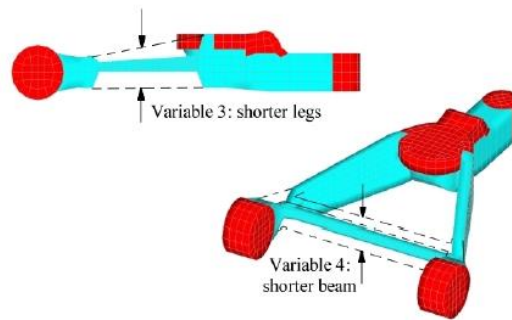


Figure 28.2 Shape variables controlling the height of the control arm rear beam [10]

Topography optimization will divide these shape variables into smaller variables that control the height and thickness of sections of each leg. The type of pattern grouping selected for each variable is used to control the way that the variables get divided. Pattern grouping enhances the ability of Topography optimization to affect the shape of solid models. Without pattern grouping, the distance that a grid is allowed to move must be less than the distance to the nearby grid or elements will get turned inside out. With pattern grouping, the movement of several grids can be linked together so that those grids can move far beyond their original positions while still maintaining a reasonable element mesh.

Since shape variables are being assigned to topography, the height and the bounds in the DTPG card do not need to be defined, as they are controlled by the shape variable. Even if these values are defined, the software will ignore them.

The objective for the optimization was to minimize the mean compliance of the control arm for all three load cases combined. The mass of the control arm was constrained to be less than 10% below its initial mass. The software generated the following solution (see Figure 28.3). The red shows areas where material was added, the blue shows areas where material was removed.

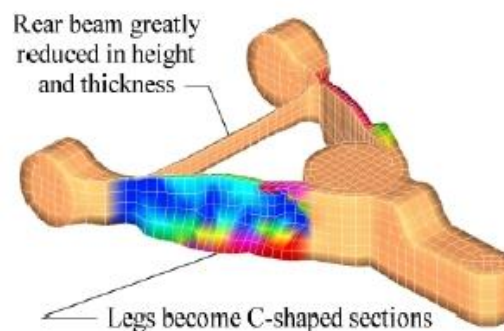


Figure 28.3 Optimized control arm using Topography and user-defined Shape variables [10]

Optimized solution shows the shape of the legs by shifting mass from the center to the top and bottom, creating C-shaped sections. These sections add vertical bending stiffness while leaving the shear and axial stiffness intact. Additionally, the height of the legs was increased along their length to further increase the bending stiffness of the sections. The size of the rear beam in both height and thickness results greatly reduced, indicating that it was oversized or perhaps even unnecessary. Overall, the maximum deflection for all three load cases was reduced by 5% while the mass was reduced by 10%. Figure 28.4 shows a refined finite element model of the software solution.

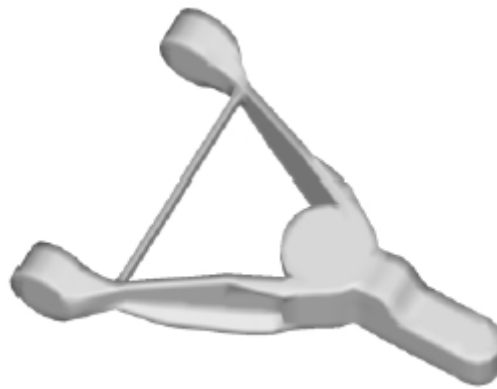


Figure 28.4 Finite element model of the OptiStruct solution [10]

Comparing these results with results of Topography without defining shape variables (chapter 1.3.1.2) is clear that now the time to set the optimization grows significantly, but it is also possible to interpret the result much easier with OSSmooth.

1.3.2.3 Free-Shape

Free-Shape optimization is different from other shape optimization techniques because the allowable movement of the outer boundary is automatically determined avoiding definition of shape perturbations. Free-Shape design regions are identified through the definition of DSHAPE bulk data entry and are specified by the grids on the outer boundary of the structure; the edge of a shell structure or the surface of a solid structure. Design grids are free to move in one of two ways shown in fig. 29 during Free-Shape optimization, the normal directions change with the change in shape of the structure, therefore the design grids move along the updated normal for each iteration. Design regions should be selected where structure could be most sensitive to the concerned responses (e.g. selecting grids in a high stress region when the objective is to reduce stress). It is possible to define different design regions to be sure that desired zone changes independently.

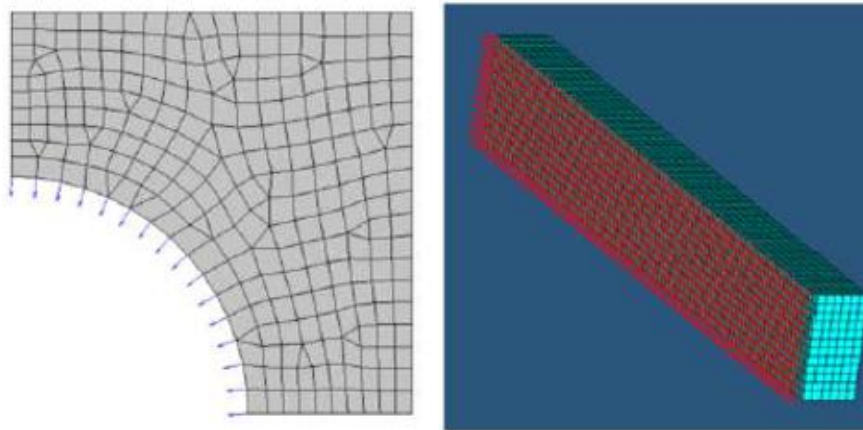


Figure 29 Left: For shell structures, grids move normal to the surface edge in the tangential plane; Right: For solid structures, grids move normal to the surface [10]

Now parameters that affect the way in which the free-shape design region deforms are reported. Those are defined on the PERT continuation line of the DSHAPE as shown below:

(1)	(2)	(3)	(4)	(5)	(6)	(7)	(8)	(9)	(10)
	PERT	DTYPE	MVFACTOR	NSMOOTH	MXSHRK	MXGROW	SMETHOD	NTRANS	

Direction Type provides a general constraint on the direction of the movement of the free-shape design region. DTYPE has three distinct options (fig. 30):

1. GROW – grids cannot move inside of the initial part boundary.
2. SHRINK – grids cannot move outside of the initial part boundary.

3. BOTH – grids are unconstrained.

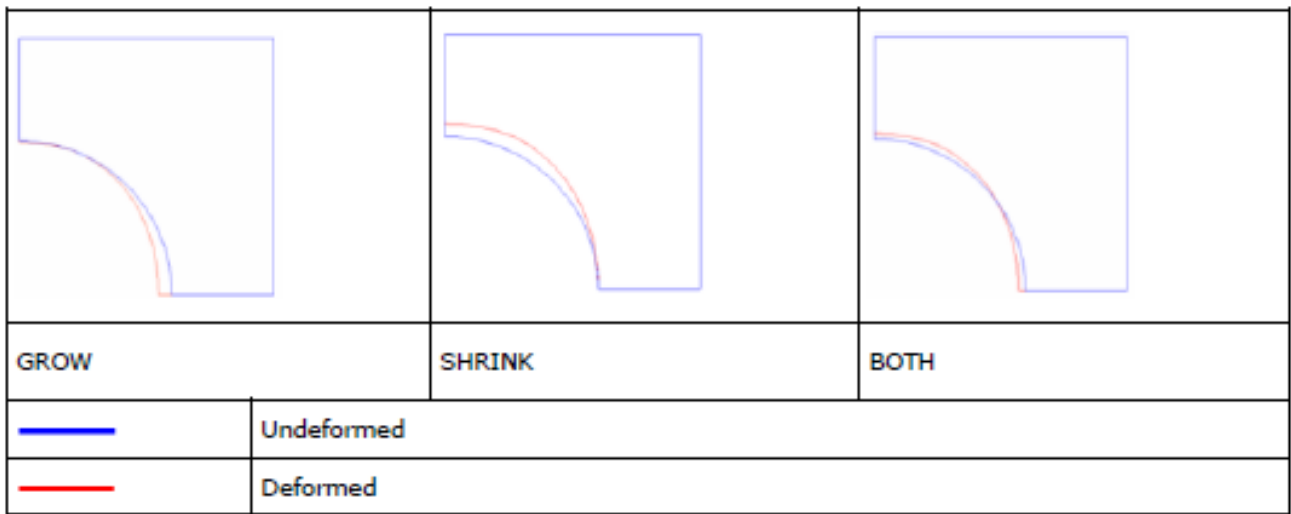


Figure 30 Direction Type definition [10]

Move Factor affects the maximum movement in one iteration and is the maximum allowable movement in one iteration of the grids defining a free-shape design region is specified as: **MVFACTOR** * mesh_size. With mesh size like the average mesh size of the design region (fig. 30.1).

The default value of MVFACTOR is 0.5. With a smaller MVFACTOR optimization run slower but with more stability. With a larger MVFACTOR optimization run faster but with less stability.

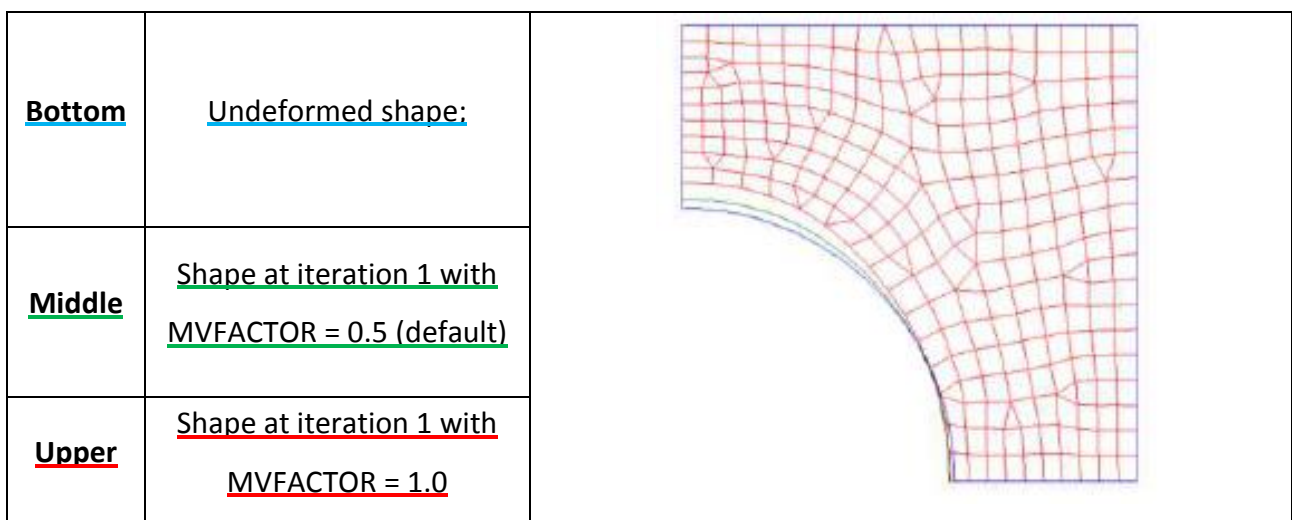


Figure 30.1 Move Factor definition [10]

Internal grids adjacent to those grids defining the design region are moved to avoid mesh distortion. The number of layers of grids to be included in the mesh smoothing buffer may be defined by the **NSMOOTH**. The default value of NSMOOTH is 10. A larger NSMOOTH will give a larger smoothing buffer avoiding mesh distortion but resulting more time consuming.

The maximum shrinkage (**MXSHRK**) and growth (**MXGROW**) limit the deformation of the design region that is defined by two barriers as shown in Fig. 30.2. The design region is then constrained to deform between these two barriers.

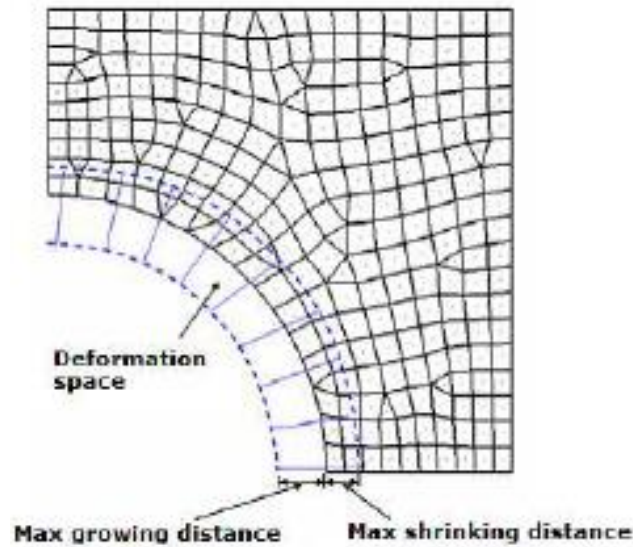


Figure 30.2 MXSHRK is the offset in the shrinkage direction and MXGROW is the offset in the growth direction.

Deformation space defined by the maximum growing/shrinking distance [10]

NTRANS helps to smooth out the transition between non-design area and design zone defining the number of design grid layers in transition zone (fig. 30.3).

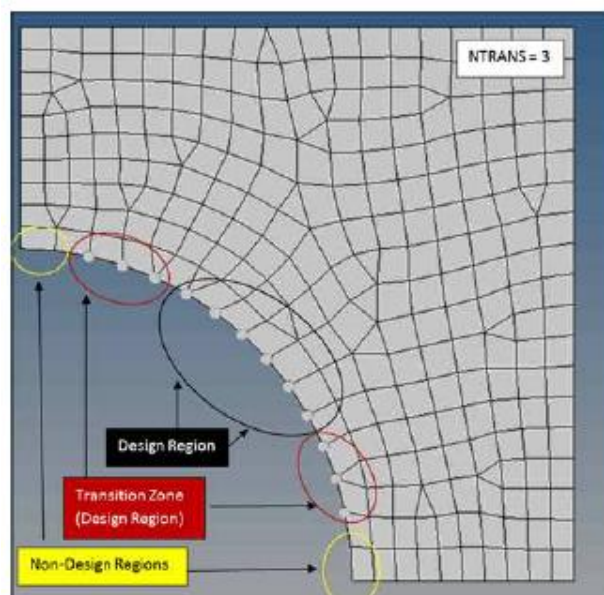


Figure 30.3 Defining the Transition Zone grid points for a smooth transition between Design and Non-Design regions (NTRANS=3) [10]

Mesh Barrier Constraints is used to limit the extent of the total deformation of the design region. The mesh barrier is composed of special shell elements (BMFACE). The mesh barrier is defined on the BMESH continuation line (fig. 31).

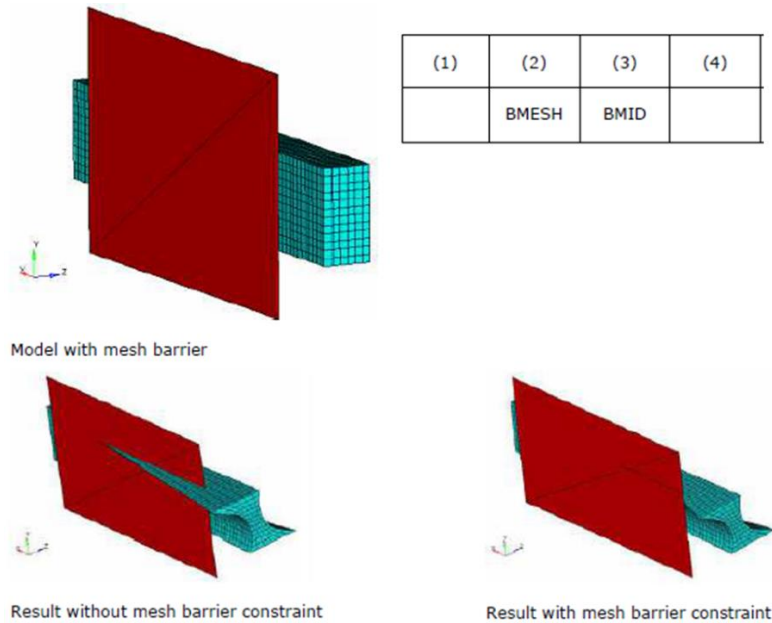


Figure 31 Example Showing Mesh Barrier Constraint [10]

In the next example (fig. 31.1), the objective is to minimize the Von Mises stress subject to a volume constraint using Free-Shape optimization. A **circular extrusion** path is defined using a cylindrical coordinate system. Results are shown with and without extrusion constraints (circular).

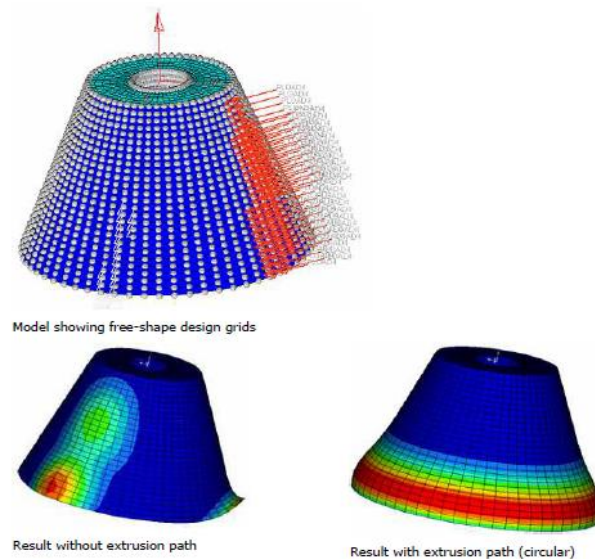


Figure 31.1 Example Showing Extrusion Constraint Along a Circular Path Example Showing Maximum Shrinkage and Growth Parameters [10]

Now is reported an example of cantilever beam with shrinkage and growth parameters. In fig. 31.2 on the right a **symmetry plane** constraint has been implemented.

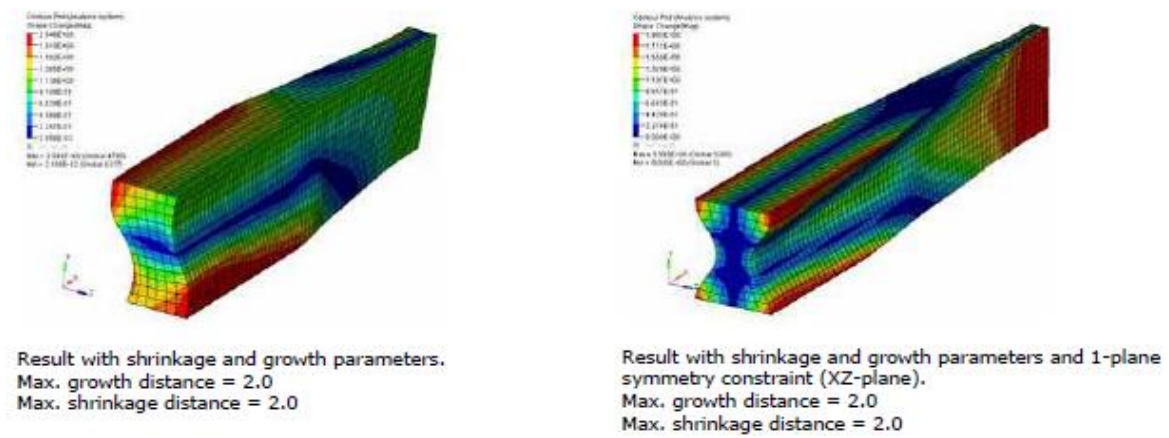


Figure 31.2 Beam with and without 1-plane symmetry constraint [10]

Comments [10]

1. When multiple constraints are defined for the same design region, while the optimizer tries its best to satisfy all the different constraints, it is possible that it may not be able to coordinate all these constraints.
2. If constraints like mesh barrier, maximum growth and shrinkage, or side constraints are applied, to avoid the interference between structural parts, the constraints should be defined in such a way that clearance is guaranteed under manufacturing tolerance and structural deformation. In other words, the barrier surface should contain an offset from the potentially interfering parts.

2. Aim of the activity

The aim of the current activity is to develop a solid methodology to optimize complex aviation components maximizing the benefits of AM process.

Components are different from each other, with own boundary conditions, their work conditions, their kind of loads (static and/or dynamic). Anyway, a frequency analysis is always requested to be sure that frequency of applied loads is far from frequencies corresponding to natural one of the structure.

It is clearly impossible to consider entire model connected to the object of optimization but consider boundary conditions in precise way is a necessity. For this reason, reduction has been developed and has been taken into account during the simulation of the real test case.

Another point analysed is the possibility to follow different ways of structural optimization. It is possible decide for static and/or dynamic optimization. Furthermore, using optimization instruments it is possible simply improving existing components, modify a specific part of the component called Design Space or redesign entire component.

For this thesis, special consideration has been done for redesign an aircraft component that present behaviour to be thin. For these reasons it will be considered both to optimise a thin surface and both redesign a design space disengaging from thin wall, then it is considered how to cover the part to reach the constraint of closed part.

During redesign process, AM constraint like minimum thickness of the wall, overhang angle in a way that part could be produced with less supports as well and tubes self-supported, have been considered.

Optimizations mentioned in literature are considered and a guideline for optimize components to reach typical objective has been developed. This guideline is obtained considering AM process but could be considered useful also for other kind of processes depending on the problem or just doing an accommodation.

To realize those purpose have been used some commercial software:

- CAD software to build design and non-design space;
- FEM software to reduce components;
- Structural optimization software to design or re-design aircraft components;
- Another CAD software that allow to build polynurbs features.

3. Design for Additive guidelines

Nowadays the design methodology has been radically changed thanks to Additive Manufacturing. During preliminary design is useful investigate more solutions as possible without traditional manufacturing constraints. For these reasons optimization instrument is necessary. In this chapter a methodologic approach to optimize components it is presented. This methodology has been developed thanks to the exercise of optimization of an Housing belonging to a turboprop engine. These guidelines are recommended for redesign and optimize an already existing component but could be used also for an ex novo component with due changes.

The optimization process can be divided in three sub problems:

- Problem Definition;
- Design Optimization;
- Design Validation.

3.1 Problem Definition

Problem Definition is the first phase to optimize a component and consists to understand its functionality and criticality; then carefully define a baseline. The baseline had its loads, boundary condition (constraints and working condition) and own feedbacks for instance in terms of frequencies and/or displacements. Once baseline is defined, loads and boundary conditions are considered fixed during optimization.

3.2 Design Optimization

The proposal Design Optimization phase could be defined by following steps:

1. Define Design, Non-Design Space and responses;
2. Explore possible Conceptual Design optimization suitable for the case study;
3. Choose the most promising;
4. Interpret results and re-analysis;
5. If results are satisfactory keep going to Design Validation process (chapter 3.3);
6. If results are not satisfactory run a second loop optimization exploring both conceptual and Design Fine-Tuning optimization;
7. Return to step 3.

In this chapter step 1 has been introduced but detailed explanation has been done during exercise of optimization. During this step a working domain has to be defined. The domain is composed by two spaces, Design Space and Non-Design Space. Just the Design Space is affected by optimization process and it is built in a proper way depending on kind of optimization. This will be demonstrated in chapter 6. Non-Design Space is characterized by assembly interfaces and functional geometries of original component. Responses need to be controlled during the optimization, deciding which of them is constrained and which is chosen as objective. In this phase it is possible to relax or tighten up the constraint compared to the baseline.

Step 2 could be done by consulting chapter 1.3 and experimenting in a way to become confident with optimization instruments.

Step 3 consist of a natural choice of the optimization that give more interesting results.

Step 4 is characterized by postprocessing results of optimization and when geometry is permissible smoothing process can start. Smoothing process consists to re-analysis of optimized geometry checking results and then move on to the re-building geometry. The re-building is done subsequently because it is time consuming process.

Notice that not all behaviours of the component could be optimized at the same time because of the structure of the optimization problem; sometimes could be necessary a loop approach. For this reason, during definition of steps in points 5 and 6 is chosen word "results" and not "responses". As instance if displacements are the constrained responses in the step 1 and displacements have been respected by re-analysis of step 4 it is possible investigate other component behaviours, e.g. stresses, that need to be monitored and be acceptable. If these other behaviours ("results") are acceptable, the Design Optimization could be stopped (step 5), vice versa there is a need to keep going to the step 6 trying to obtain satisfactory results.

Now an example of Design Optimization from step 1 through step 5 focused on smoothing process for Topology optimization is shown in fig. 32.

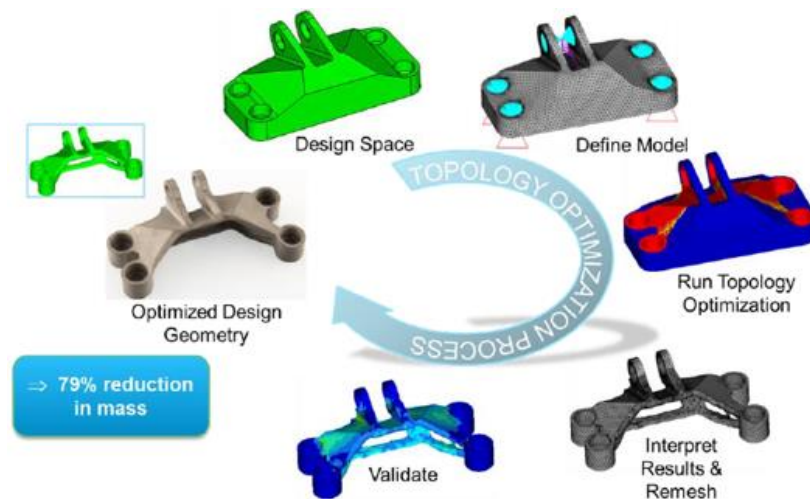


Figure 32 Description of the topology optimization process; jet engine bracket shown as an example [13]

3.3 Design Validation

After the design have been deemed to be printable, the task of finalizing the design need to be undertaken. Design Validation is the last phase of optimization process and consist to submit component to different analysis. The first analysis usually done is a static one with second order mesh elements in order to evaluate stresses more accurately. Other tests are set up according to business practice as stress test, limit and ultimate test, LCF and HCF. Once the design show that it would meet all specifications, the corresponding STL file need to be imported into suitable software to prepare for printing describing orientation of the part on the build platform and by providing required supports [13].



Figure 33 Design Validation Left: Structure submitted to different analysis; Right: Addition of supports [13]

4. Exercise of Topology optimization with Overhang constraint

From literature are clear the issues related to have overhang features in components produced with AM process. For this work thesis the manufacturing constraint of overhang for Topology optimization has been used thanks to the availability in the last version of the available software. So, in this section an exercise is reported to demonstrate limits and strength of the overhang constraint. It permits during phase of conceptual design to decide grow direction and angle between grow direction and solid parts, the penalization scheme and choice between supported and self-supported building. Therefore, overhang constraint could be defined as a limit angle that solid geometry builds layer by layer has respect the grow direction (fig. 33).

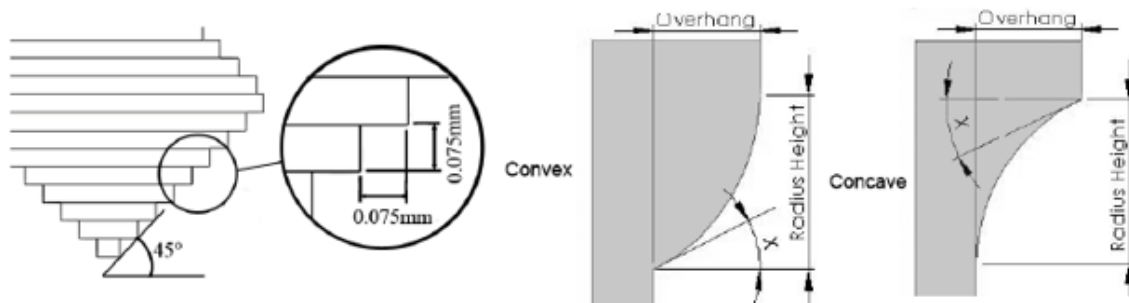


Figure 33 Left: Illustration of the 75µm maximum layer overhang at 45°; Right: Convex and Concave example.

Setting supported geometry in the software, results need to be interpreted. Usually there are a lot of study that concern the theory of support and require thermal stress monitoring. For these reasons in this exercise is considered just a self-supported option and thermal stresses are not considered. By choosing self-supported option and knowing the limit angle that allow the considered material to avoid supports, the obtained geometry may be considered manufacturable.

There is a possibility to choose one of two most popular approaches to penalize densities in Topology optimization with overhang constraint, Solid Isotropic Material with Penalization (SIMP) and Rational Approximation of Material Properties (RAMP). These approaches use interpolation schemes to force the density values to go to the bounds.

A dummy cantilever beam has been developed as shown in Table 5.

In Table 6 Topology optimization without overhang constraint is represented. Instead, in the Table 7 Topology optimization with manufacturing constraint of overhang is reported with the same value of threshold densities.

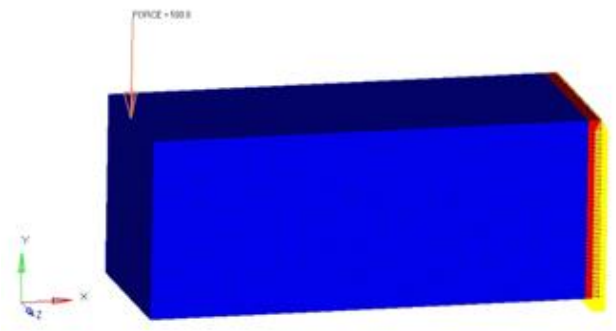
Geometry	Length = 100 [mm]; Height = 40 [mm]; Width = 40 [mm];	
Material	Inconel	
Loads	FY 500 [N]	
Constraints	Nodes of right surface	
Elemensts	3D solid elements	

Table 5 Dummy cantilever beam definition

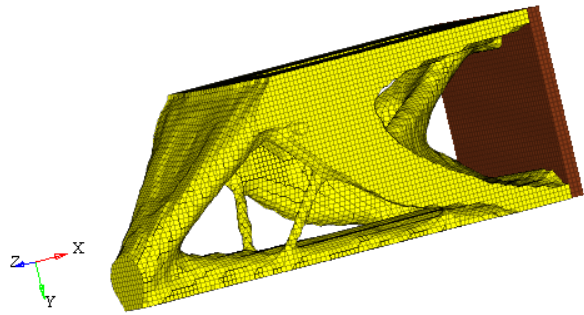
Topology Optimization	Without Overhang Constraint	
Objective	Min Comp	
Constraints	Volfrac 0,25 (-75%) Disp. Constr. 1 [mm]	
Result Comp	5,981 [Nmm]	

Table 6 Topology optimization without overhang constraint

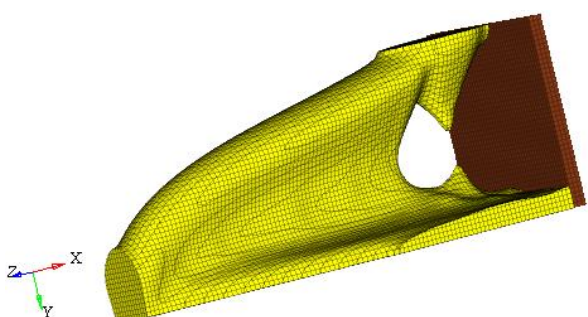
Topology Optimization	With Overhang Constraint Self-supported (grow direction -Y)	
Objective	Min Comp	
Constraints	Volfrac 0,25 (-75%) Disp. Constr. 1 [mm]	
Result Comp	8,860 [Nmm]	

Table 7 Topology optimization with overhang constraint

A lot of solutions have been investigated changing parameters allowable for the overhang constraint before to reach this result. Different kind of problems, understood as geometry, or different combination of parameters like MINDIM are implemented. The result displayed in Table 7 are the best compromise in terms of compliance once overhang constraint has been introduced. As expected an increase of compliance respect to standard topology optimization without overhang constraint. Anyway, an increase of compliance happens every time that constraints have been increased or a manufacturing constraint is introduced.

5. Exercise of Optimization on Dummy Conical Housing

When a component is analysed it is important to understand its static and dynamic behaviours. In this chapter a dummy conical housing is developed keeping in mind the optimization problem on real test case. According to chapter 3 about guidelines, here Problem Definition and Design Optimization are investigated; Design Validation is not considered.

5.1 Problem Definition

In this exercise is supposed that on the node of application of loads are applied static and dynamic loads along X direction (positive and negative) and that lower ring surface of bottom flange is constrained. For this reason, firstly a static analysis has been done, then a modal analysis and lastly a Frequency Response Function (FRF). Results of baseline model thus defined are then considered for the optimization problem.

Geometry and Finite Element Model (FEM) for static analysis are shown in table 8.

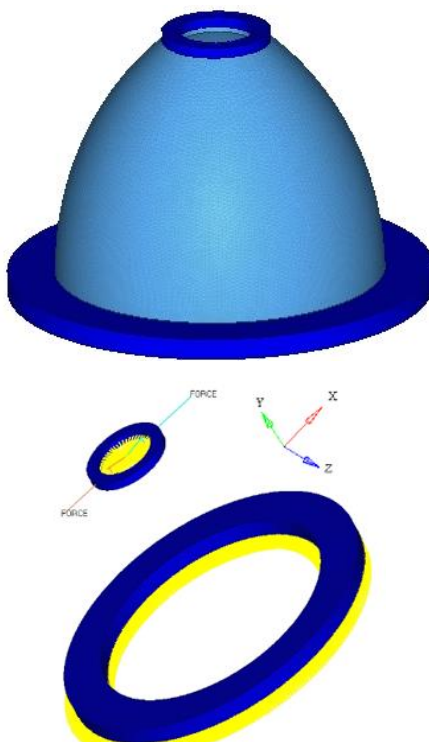
Geometry	base diameter = 80 [mm]; Height = 110 [mm]; Thickness = 2[mm];	
Material	Steel;	
Loads	On center node of RBE3 elements connected to upper flange: FX = 50 [kN]; -FX = 50 [kN];	
Constraints	Lower ring surface of bottom flange are fixed;	
Elements	3D solid elements on interface rings and 2D shell elements on conical surface,	

Table 8 Geometry and FEM model of dummy conical shape

Notice that conical shape of baseline could be discretized by shell elements or by a huge amount of 3D elements because of the thin thickness and it is a good practice to have 3 elements for each

thickness. Obviously shell discretization run faster. For these reasons in this study 3D discretization of baseline shape has not been considered.

Useful values and results from static analysis are reported in table 9.

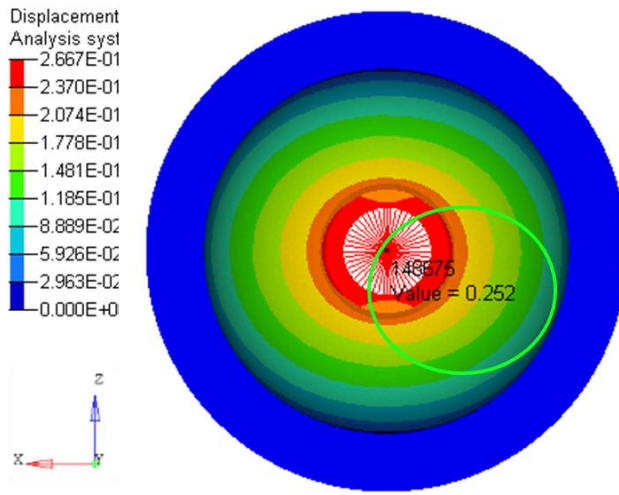
Mass	Interfaces = 0,57 [kg]; Cone = 0,48 [kg]; Total = 1,05 [kg];	
Disp.	<u>RBE3 center = ±0,25[mm];</u>	
Comp.	Total = 6,29e+03 [Nmm]	

Table 9 Entities useful and displacement result of static analysis

Subsequently modal analysis is done keeping constrained the lower ring surface so that are not observed rigid mode ($\omega_n = 0$). A Modal Participation Factor (MPF) is requested to the analysis with command PARAM, EFFMASS, YES:

$$[mpf] = \frac{[\Phi]^T [m] [\alpha]}{[M]};$$

With:

- $[\Phi]$ is eigenvector matrix;
- $[m]$ is mass matrix of the system;
- $[\alpha]$ taken into account of directions;
- $[M]$ is the diagonal mass matrix ($[\Phi]^T [m] [\Phi]$);

MPF tells how each mode give a contribute to displacements in a specific direction when in that direction a load is applied. From modal analysis is observed that the first 15 modes (from 5 until 10 [kHz]), are sufficient to investigate the dynamic behaviour. The main modes according to MPF are mode 1, mode 2 and mode 13, respectively X, Y and Z direction (see fig. 34). In fig. 34, mode 1 is underlined because then FRF analysis is done with loads in X direction.

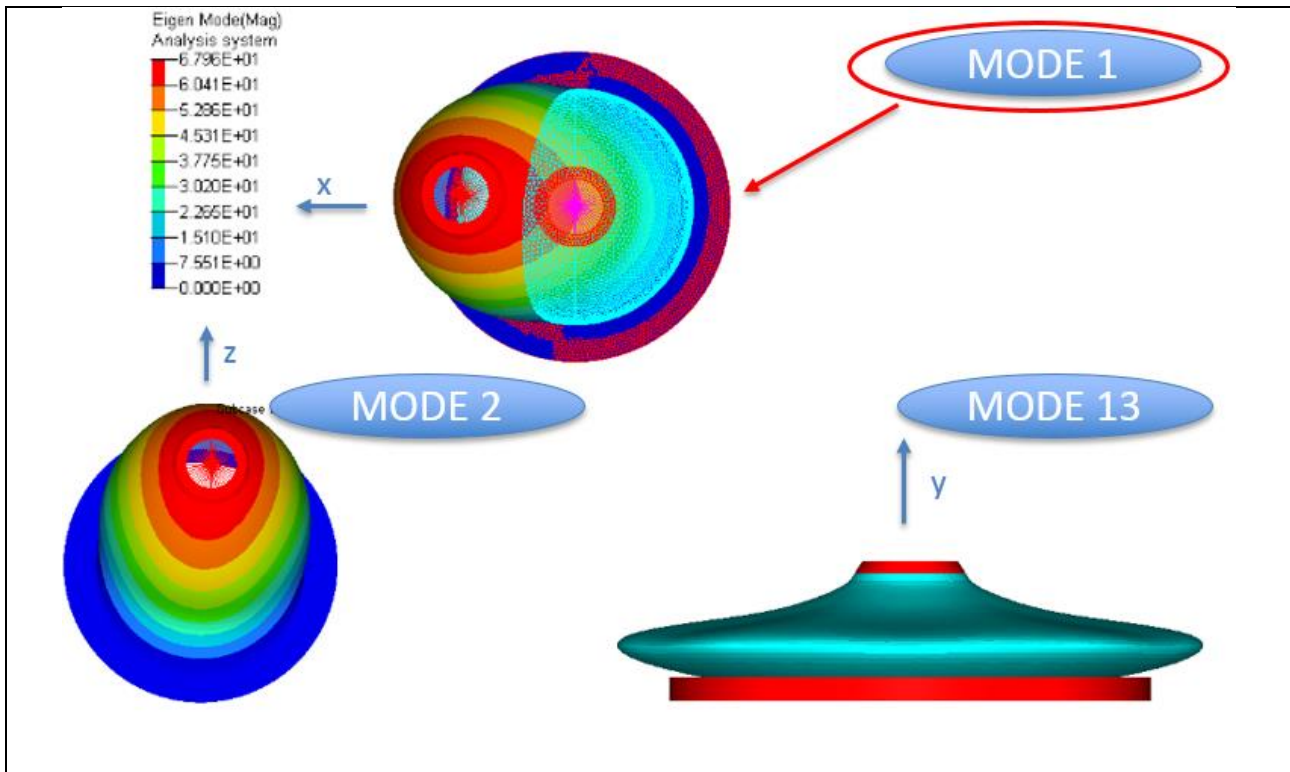


Figure 34 Modes of interest; Mode 1 is underlined because then FRF analysis is done with loads in X direction

Then FRF analysis is done considering loads in X direction, positive and negative, defined using RLOAD2 as:

$$f(\Omega) = A \cdot B(\Omega);$$

With:

- $A = 50 \text{ [N]}$;
- $B = 1 \text{ in frequency range } [0; 10] \text{ [kHz]}$;

With PARAM,G is chosen a constant damping ($G = 0,005$). It means that constant damping is 2,5 % of critical damping ratio ($\zeta = c/c_{cr}$). In fig. 35 is shown FRF plot that underline that peak is fixed for the first natural frequency as expected by the fact that load is applied along X direction; maximum displacement is 0,0038 [mm].

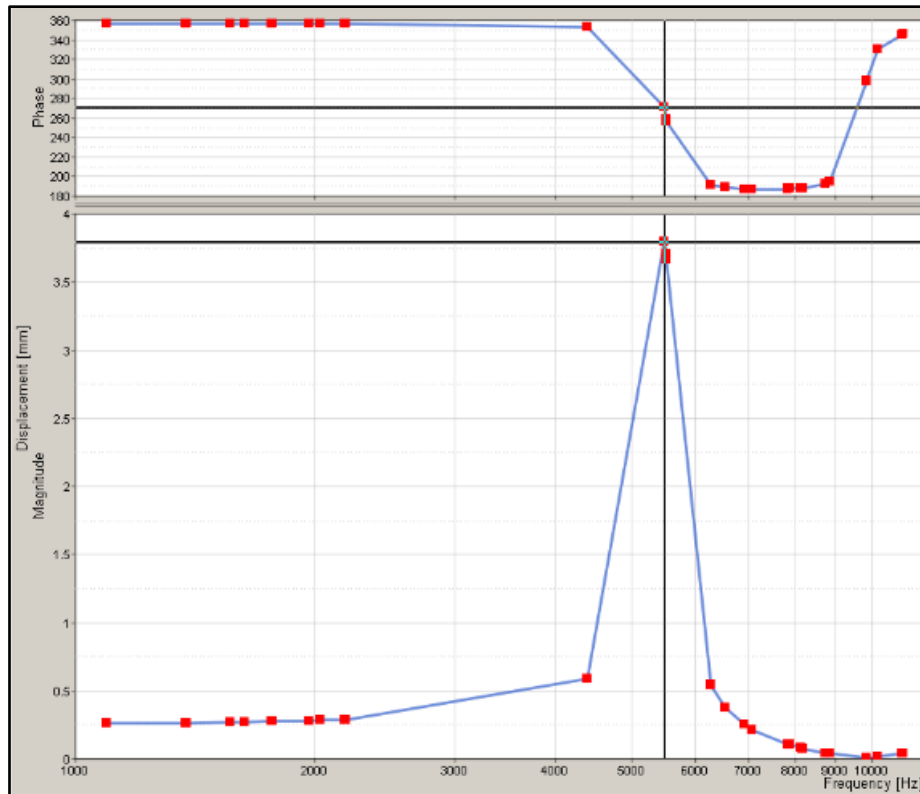


Figure 35 Value of maximum displacement of 0,0038 [mm] is observed for the first natural frequency

5.2 Design Optimization

For this case study two approaches of optimization have been followed, the first is to optimize a shape of baseline and the second is to define a new load path thanks to topology optimization done using biggest volume as possible.

1. On shell elements of baseline model two optimization have been done: Free-Size and Topography. The Shape optimization is not used in this exercise because of its needs to move nodes with HyperMorph panel that result time-consuming. Considering manufacturing process is thought that variable thicknesses are producible and so Free-Size optimization is preferred to Size optimization. It is also possible perform a Topology optimization on shell elements but in literature is explained how from Free-Size on shell elements are obtained similar result of Topology optimization on the same shape but discretized with 3D elements. Thus, Topology optimization on shell elements has not been evaluated. If a discretization 3D of baseline shape is computationally possible, also a Free-Shape optimization could be done.
2. Then an increased volume has been built, thus Topology optimization is done on a new Design Space finding new load path.

So, the three Concept Design optimizations are evaluated: Free-Size, Topography and Topology. Optimizations of Design Fine-Tuning could be applied to results of those but for this dummy case study the optimization exercise stops to conceptual phase (step 2 considering 3.2).

In this optimization there are static displacement, dynamic displacement and mass constrained. The first two responses are constrained at the baseline value. The mass is constrained to be reduced of 10% compared to baseline. As objective a minimization of weighted compliance is imposed.

$$\textit{Weighted Compliance} = \sum W_j C_j;$$

Where j is the index of load subcase, C is the Compliance and W is the weight associated to each subcase.

For the following three optimizations responses, constraints and objective shown in tab. 9 have been kept fixed.

Objective	Minimize Weighted Compliance
Static Displacements constraint	RBE3 center = $\pm 0,25$ [mm];
Dynamic Displacements constraint	RBE3 center = $\pm 0,0038$ [mm];
Mass constraint	0,95 [kg] (-10%);

Table 9 Constraint and objective of optimization shared by optimizations considered

5.2.1 Free-Size static-dynamic 2D

For Free-Size an initial thickness on PSHELL property has been assigned. Thanks to this optimization there is the opportunity to choose min and max thickness that software considers as limits (see tab. 10).

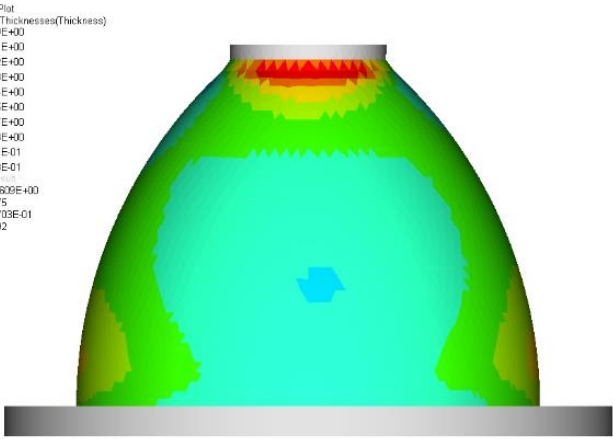
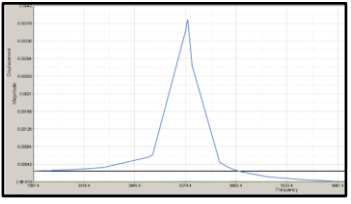
Thicknesses	$T = 4,0 \text{ [mm];}$ $T_{\min} = 0,4 \text{ [mm];}$ $T_{\max} = 4,0 \text{ [mm];}$	
FRF		
Comp. Result	Total = $6,29\text{e}+03 \text{ [Nmm]}$ (baseline)	

Table 10 Free-Size results, contour plot of variable thicknesses

5.2.2 Topography static-dynamic 2D

To reach mass reduction of 10%, for Topography optimization is advisable starting from reduced value of thickness comparing it to baseline one because during simulation movements of nodes is expected and mass shall be increase. Notice that for this optimization it is possible to choose following parameters discussed in literature: min width, draw angle, draw height.

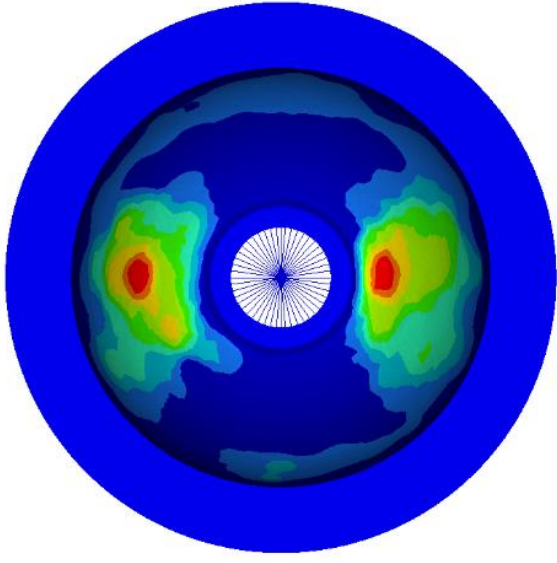
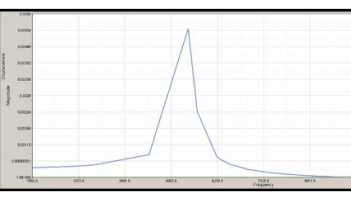
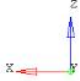
Thickness	$T = 1,5 \text{ [mm];}$	
Topography parameter	min width = 8 [mm]; draw angle = 60 [°]; draw height = 10 [mm];	
FRF		
Comp. Result	Total = $8,15\text{e}+03 \text{ [Nmm]}$ (+23,0%)	

Table 11 Topography results, contour plot of shape change

5.2.3 Topology static-dynamic 3D

With Topology optimization have been introduced optimization parameter like MINDIM (manufacturing constraint that allows to choose size of members), MATINIT (is the initial value of mass because of starting volume is widely large), MINDENS (to avoid lability) and DISCRETE (is related to penalization factor).

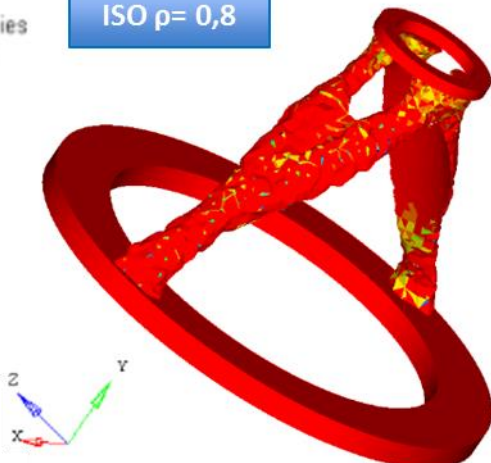
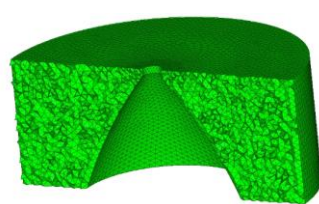
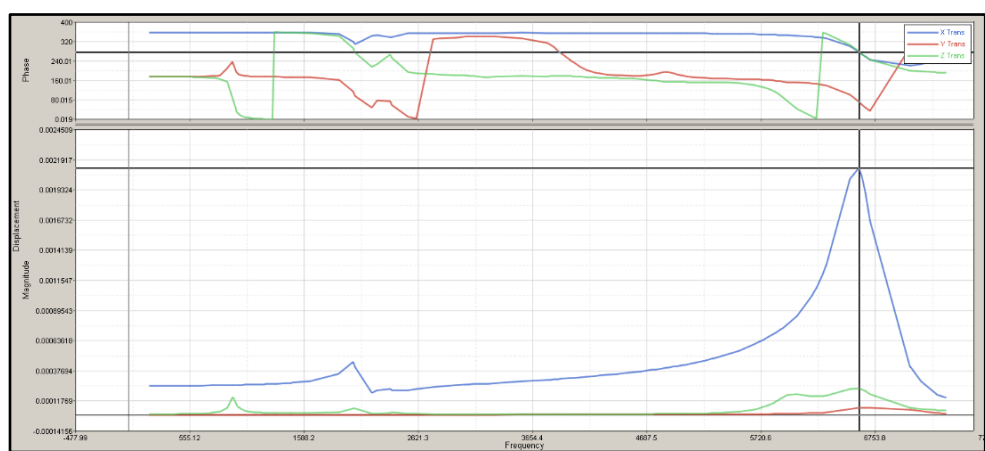
Optimization parameter	MINDIM =12 MATINIT = 0,3 MINDENS = 0,001 DISCRETE = 3	<div>Contour Plot Element Densities</div> <div><div>1.000E+00</div><div>8.830E-01</div><div>7.780E-01</div><div>6.670E-01</div><div>5.560E-01</div><div>4.450E-01</div><div>3.340E-01</div><div>2.230E-01</div><div>1.120E-01</div><div>1.000E-03</div></div> <div>ISO $\rho= 0,8$</div> 
Design space		
Comp. Result	Total = 6,15e+03 [Nmm] (c.a. baseline)	
FRF		

Table 12 Topology results, contour plot of densities values

The geometry compared to the baseline is completely changed thus that MPF is different and the peak of FRF is observed for 6,6 [kHz] instead of 5 [kHz]. Furthermore, the peak is 0,0021 [mm] instead of 0,0038 [mm]. Notice that peaks in other direction are now present.

5.2.4 Conclusion of Conceptual Design

By this exercise, main differences between three Concept Design optimization and kind of discretization request, have been understood. By optimizations results is evident that constraining mass to be reduced of 10%, FRF is quite the same of the baseline for Free-Size and Topography but change in Topology; compliance increase in Topography and decrease a while in Topology. It would be possible to investigate more to reach best solutions but for this test case has not been considered necessary. The Topology is major investigated in this thesis because it is considered a powerful instrument for re-design most of components keeping in mind the AM process. Therefore, more parameters are implemented for Topology optimization, indeed the best result is found for this simulation. At this point the phase of Conceptual Design could be considered concluded and for this dummy exercise we stopped at the third step defined in 3.2 choosing the Topology optimization as the most promising.

Moreover, this exercise has been useful to understand better how dynamic responses work because in literature there are not a lot of practice cases with these kinds of responses. Different simulations with different responses as constraint or as objective have been done. Some considerations that could be useful with dynamic optimizations are now underlined. For normal modes analysis there are responses that could be chosen for each loadstep (Frequency; Mode Shape) and there are responses that consider all loadsteps. In particular, there is “weighted frequencies” for dynamic loadsteps and “combined compliance index” for dynamic and static loadsteps that is a combination of weighted compliance and weighted frequencies.

$$\textit{Weighted Frequencies} = \sum \left(\frac{W_i}{\lambda_i} \right) ;$$

Where i is the index of frequencies, λ is the frequency and W is the weight associated to each frequency.

$$\textit{Combined Compliance Index} = \sum W_j C_j + \textit{NORM} \left(\frac{\sum \left(\frac{W_i}{\lambda_i} \right)}{\sum W_i} \right);$$

For Frequency Response Function analysis for each loadstep can be chosen a response like FRF displacement, FRF acceleration etc. Instead there is not a response that could be minimized considering more dynamic loadsteps. Notice that optimization problem could be customized but this has not been investigated.

6. Exercise of Optimization of a Turboprop Engine Housing

This chapter is turned to optimize an industrial test case thanks to which the method has been improved and proposed in chapter 3. The object of the study is a Housing of a Turboprop engine that has structural functionality. According to design for additive guidelines firstly Problem Definition then Design Optimization and lastly Design Verification have been defined. The component has been optimized keeping in mind the baseline with the main objective to reduce weight as in any aerospace case study. When it is possible other targets, like stress peak, has been monitored.

6.1 Problem Definition

Here are presented the main behaviour of the engine, workings of Planetary Gearbox and functions of the Housing. Subsequently a baseline has been defined; boundary conditions, loads, reference displacements and reference stresses.

6.1.1 Introduction to Engine

Analysed Housing belong to a Turboprop engine composed of:

- Accessory Gearbox (AGB);
- Air intake and nozzle;
- Gas generator that consist of high pressure compressor, combustor, high pressure turbine;
- Free power turbine released by the gas generator;
- Exhaust;
- Planetary Gearbox (PGB) between free power turbine and propeller;

These components are inside a static structure (engine nacelles) connected to hardpoint as shown in a schematic representation in fig. 36 and fig. 37.

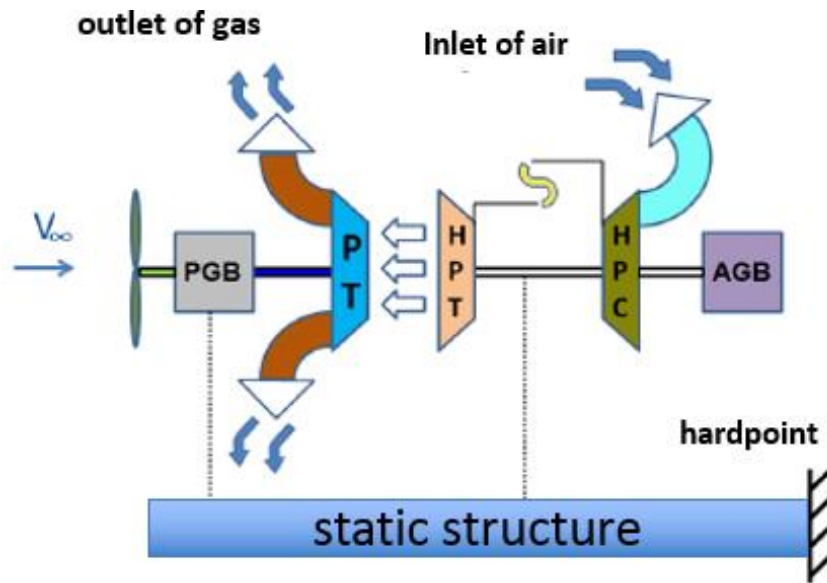


Figure 36 Left: schematic representation of a turboprop engine

In a Turboprop engine air moves through the components by reverse flow (see fig. 37). The inlet of air is behind, near to AGB. The air flow goes through air intake, high pressure compressor, combustor then in high pressure turbine. The last one sends gas to power turbine that gives motion to PGB. The outlet of gas occurs through the exhaust before of PGB.

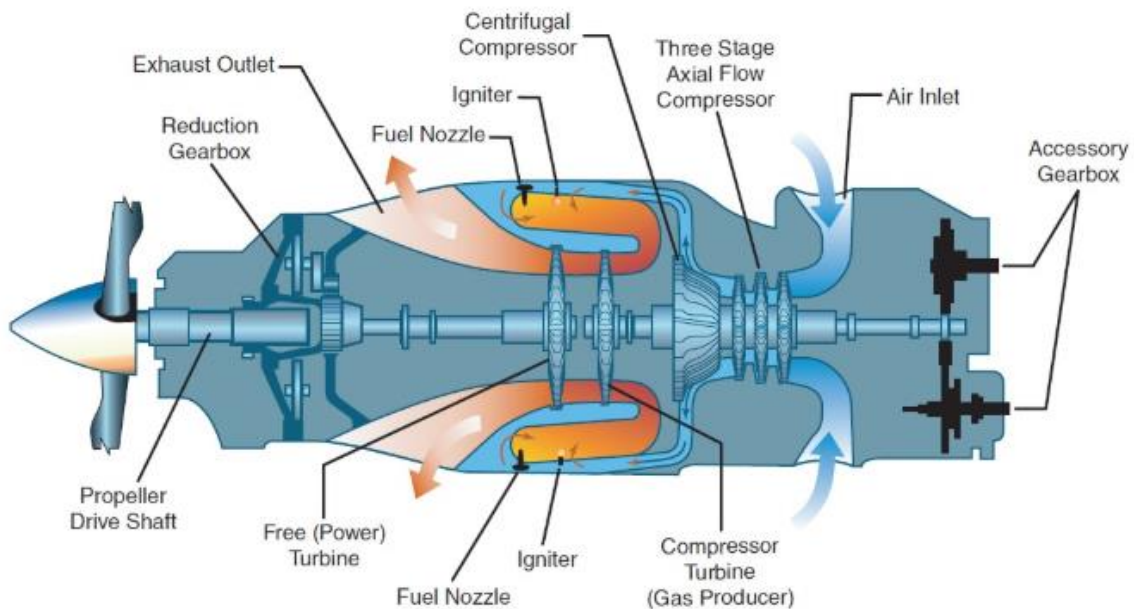


Figure 37 Schematization of reverse airflow [42]

Workings of the PGB

A planetary gearbox (PGB) is a gearbox with the input shaft and the output shaft aligned. A planetary gearbox is used to transfer the largest torque in the most compact form. PGB is used to adjust rotation speed of free power turbine and therefore propeller rotation speed. The four basic components of the epicyclic gear are:

- Sun gear;
- Planetary gears;
- Planet Carrier;
- External crown;

Planet Carrier holds one or more planetary gears, all with the same size, meshed with the sun gear and with external crown that have inward-facing teeth (see fig. 38).

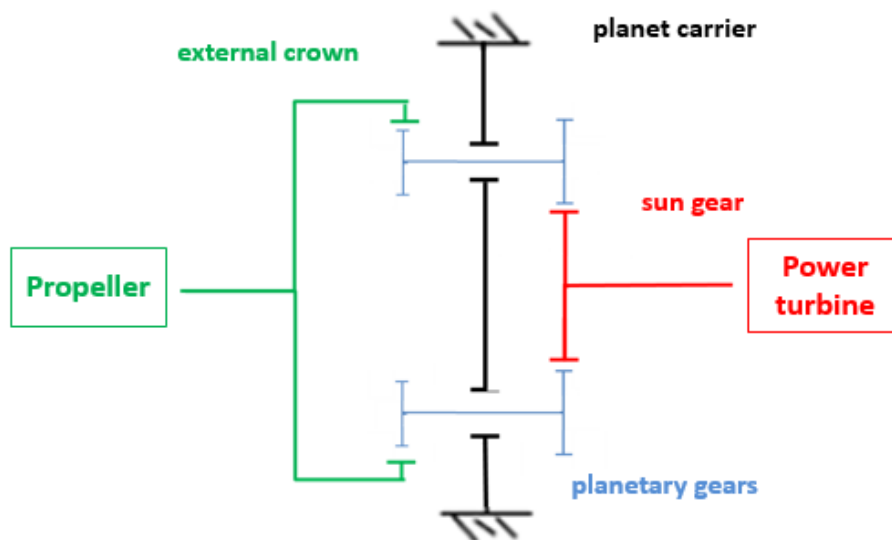


Figure 38 Schematization of a PGB

Functions of the Housing

The main functions of the Housing object of study are the following:

- Support propeller with two bearings (ball and roller) transmitting loads by upper flange to bottom flange;
- Cover the PGB;
- Support Pitch Control Unit (PCU) enabling the correct meshing of its gear with external crown of PGB;

- Tubes have to be integrated;
- Contain oil and lead this to drain on carrier;
- Allow the lubrication of bearing;

Housing is connected to others static structures through connection with carrier.

6.1.2 Baseline

In this case study baseline has been developed according with company reviews deciding which components take into account during analysis. In fig. 40 is displayed CAD model of component closest the Housing. The part that represent the exhaust is constructed approximatively. A defeaturing of very small holes and cavities has been done.

From the CAD model Exhaust, Carrier (plus rear carrier) and Housing are considered for the baseline definition. These components are meshed with HyperMesh.

For connections between Housing and Carrier as like between Carrier and Exhaust are used RBE3 elements. Nodes of the down flange of the Housing are set as independents and central node of this flange is set as dependent. This node is duplicated and an infinite stiffness between these two nodes is considered with CELAS element and PELAS property. The duplicate node is the dependent node of RBE3 on front nodes of the carrier. Similarly, Carrier and Exhaust are connected with CONTACT FREEZE. Central node of rear part of exhaust is constrained for all 6 DOFs (SPC).



Figure 40 CAD model of baseline

An aircraft structure's capability to sustain operational flight loads is commonly assessed by comparing material performance parameters to limit or ultimate loads. Limit loads are generally defined as the maximum load expected during the life of an aircraft. Ultimate loads are obtained by multiplying limit loads by the factor-of-safety that usually is 1.5. Limit loads are derived by considering the extremes of flight envelopes, gross weight, load factors, environments, and pilot inputs. In some cases, the likelihood of encountering limit load is very remote. Design criteria require structures to withstand ultimate loads without failure and limit loads with no permanent deformation [36]. For this phase of design limit loads conditions are considered as relevant one to design the Housing for static. The 7 of 48 representative limit conditions have been identified. The unbalance (rotating) loads have been added to the seven most dangerous and aligned to the most severe directions. Those loads are elaborated in an excel file obtaining resulting forces on bearings: roller and ball propeller bearings and layshaft bearings.

Bearings are simplified with RBE3 elements between dependent central node and independent node of region that have to be in contact with the external ring of bearing. Forces are applied in central node of RBE3 elements. Following company practice for radial forces that involve flexional behaviour in the structure RBE3 elements have to form a specific angle on both side respect to direction force and axial loads are applied in a way that RBE3 forms a 360 degree.

PGB loads during specific manoeuvre are transmitted to the static structures throw bearings. Thereby loads to take into account are those applied on bearings of planetary gears and on bearings of propeller (two bearings on Housing and one bearing on Carrier).

For this case study are just considered loads on front roll bearing and on ball bearing. For any loads condition are considered RBE3 elements taking care of the angles.

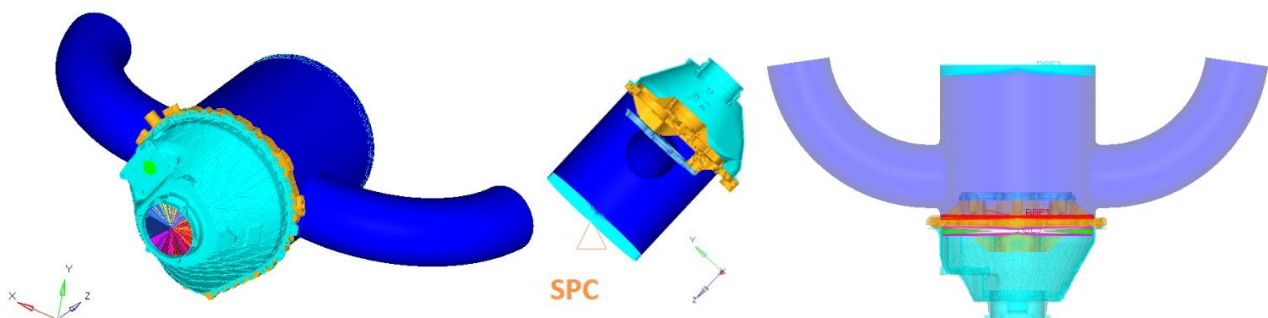


Figure 41 Baseline: Section and SPC; Connections

The following manoeuvres are imposed in each loadstep of the FEM model:

Load Step	
1	Yaw
2	Yaw mirrored
3	Vertical Static Gust Power Off
4	Max Seizure Torque
5	Yaw and Lateral Load
6	Pull-up
7	Vertical Static Gust

Table 13 Limit Load Conditions

Reduction

Nowadays reduction is useful for different kind of problems. Usually using finite element method yield models with a large number of degrees of freedom, thus could be a great advantage in reducing the size of the problem, particularly performing a dynamic analysis. Also maintain the same boundary condition result useful to obtain lighter model reducing time of computation.

For these reasons, reduced order model in the baseline model and then in the optimization simulation, have been introduced. The component of the analysis reduced is the Exhaust. Craig-Bampton method has been implemented with Nastran and with OptiStruct comparing the solutions of both software. Since static analysis only on this case study has been taken into account, the method become exactly the same of the Guyan reduction. During work thesis the method to obtain the file (.pch) to import during simulation has been done.

Therefore, all elements of the Exhaust, including RBE3 placed in front and in rear part of the exhaust are reduced at two nodes. In one node is placed Single Point Constraint (SPC) and the other node is on center of RBE3 attached to independent rear nodes of Carrier.

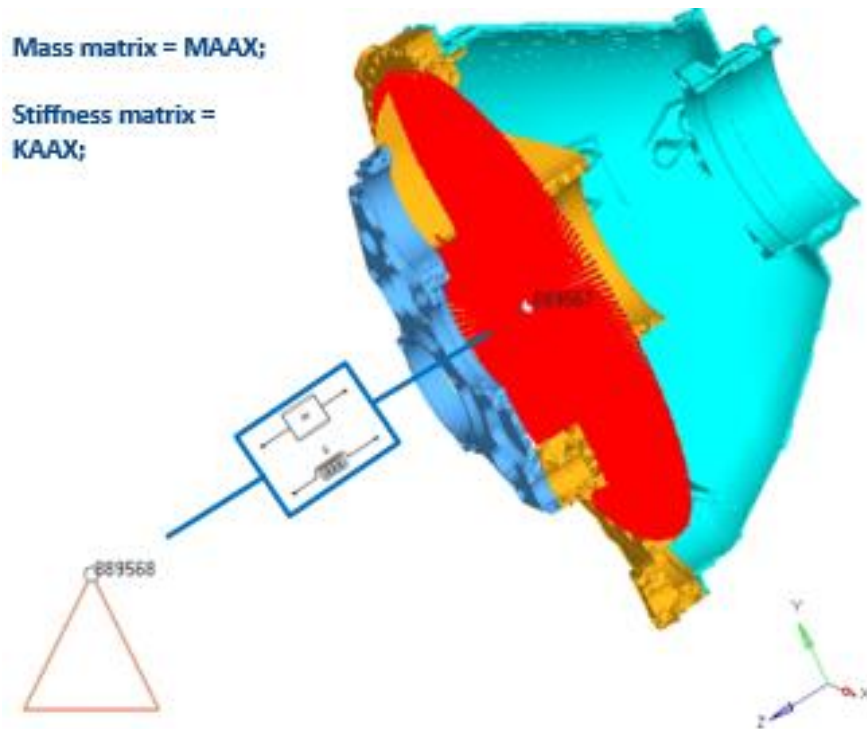


Figure 42 Schematization of ROM model of the exhaust

Baseline results

From here on we will consider just Housing to look at results. Displacements and stresses are shown in fig. 43:

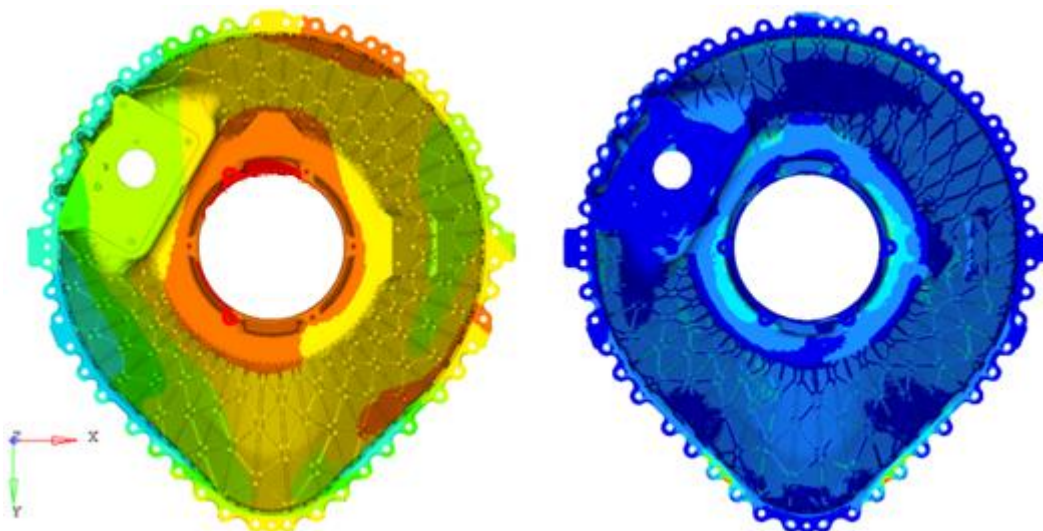


Figure 43 Displacements and stresses of the first load condition

From HyperView through node contour, displacement of center node bearing of PCU, center node of front roll bearing and ball bearing are monitored for next phase of optimization.

6.2 Design Optimization

In line with chapter 3.2 here Non-Design Space is defined; it will be useful for each of following optimizations. Then two kinds of Design Space are defined. The first one consists of mid-surface of baseline model, so that the geometry is similar to the baseline one and will be useful for some optimizations like Free-Size or Topography (Shell Design Space). The second one Design Space is an enlarged volume that is useful for Topology optimization (Design Space 3D). All necessary parts have been developed in Siemens NX.

FEM model has been built similarly to the baseline but replacing baseline housing with Non-Design and Design Space. These last two components have been linked with CONTACT FREEZE.

Values investigated are mass (set as objective), displacements (set as constraints), compliance and stresses (monitored at the end of the optimization).

Non-Design Space Definition

Non-Design Space is a defined volume of material that do not change its shape during optimization. Are considered Non-Design Space all those parts that are in contact with adjacent components not subject to optimization. Furthermore, Non-Design are the parts that need to maintain their performances. For this study these components are: bottom flange (in contact with carrier); middle flange (site for Pitch Control Unit PCU); upper flange (seat for propeller bearings); tubes (three between bottom and middle flange, one between middle and upper flange). Whereas that in first approach optimizations we want define new distribution of mass, tubes are neglected otherwise could have given stiffness between flanges. In fig. 44 is shown Non-Design Space starting from baseline.

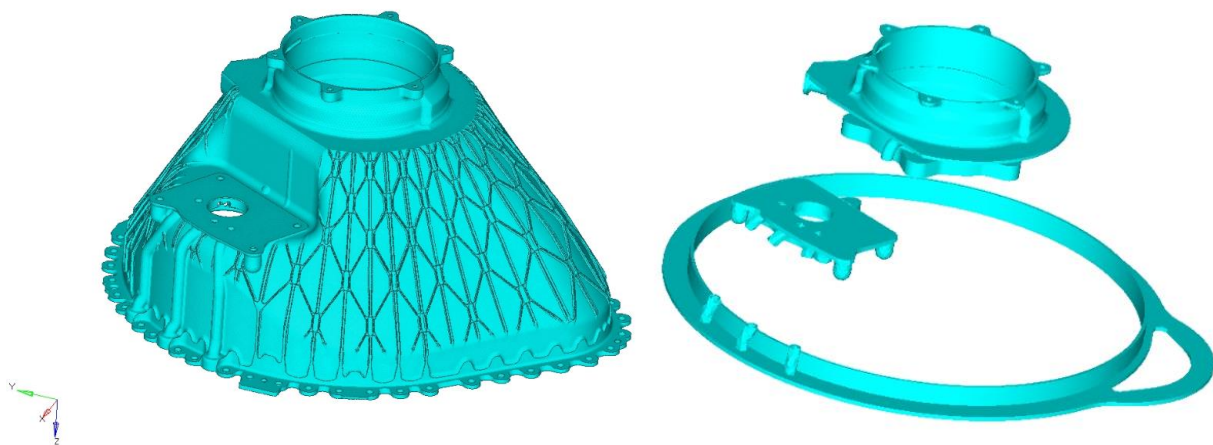


Figure 44 Extraction of Non-Design Space from baseline

Design Space Definition

The remarks made in the exercise on dummy conical shape in chapter 5 are applicable also in this case study because baseline model has thin wall. Thereby on shell elements of mid-surface are done Free-Size and Topography optimization. Being really similar to the baseline this part does not need specific considerations. Fig.45 shows Non-Design and Shell Design Space.

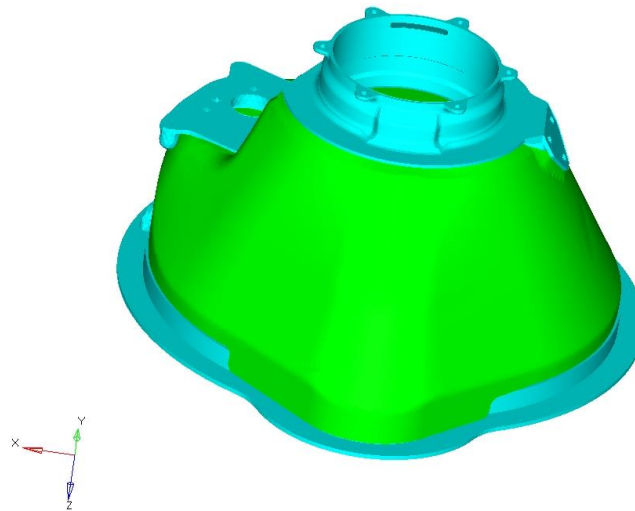


Figure 45 Non-Design and Shell Design Space

As regards Design Space increased that is useful for Topology optimization, it is built starting from the biggest volume admissible and then removing material according to assembly constraints and Non-Design Space. Emphasis has been posed for assembling Pitch Control Unit gear and bolts for Propeller. Here is shown just last Design Space volume that has been improved to accommodate material on bottom flange and has been modified to consider presence of tubes.

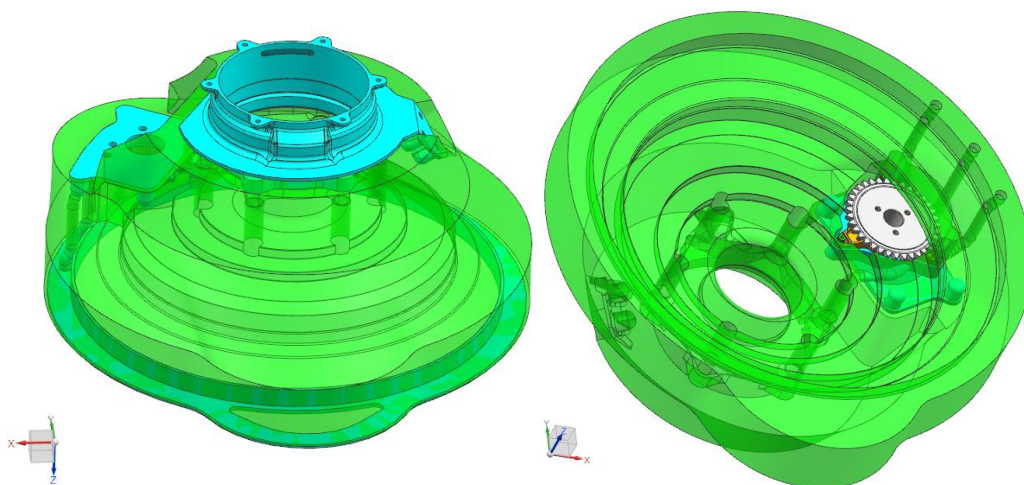


Figure 46 Left: Non-Design and Design Space 3D for Topology optimization; Middle: PCU gear; Right: Section of main parts that have been useful during Design Space construction and of Design Space

6.3.1 Free-Size on Shell Design

Free-Size optimization offers the opportunity to change thickness for each element. Starting from an intermediate thickness assigned to shell property, the solver will choose minimum and maximum thickness according to optimization parameters reaching prefixed objective. For this optimization a value of stress has been chosen as constraint by the fact that from the first attempt a high value of stress appeared in some zones. It because of stress limit need to be properly chosen in thin wall according to mechanical characteristics to avoid problems during Design Validation analysis as Fatigue analysis. The settings of optimization are shown in Table 14 and results are presented in Table 14.1. Compliance for each load condition results increased as expected by a mass reduction.

Objective	Minimize Mass
Optimization Constraints	PCU displacements (baseline) BALL displacements (baseline) ROLL displacements (baseline) Stress (55 % of UTS)
Optimization Parameters	T_min = 0,2 [mm] T_MAX = 2,0 [mm]

Table 14 Free-Size optimization on Shell Design

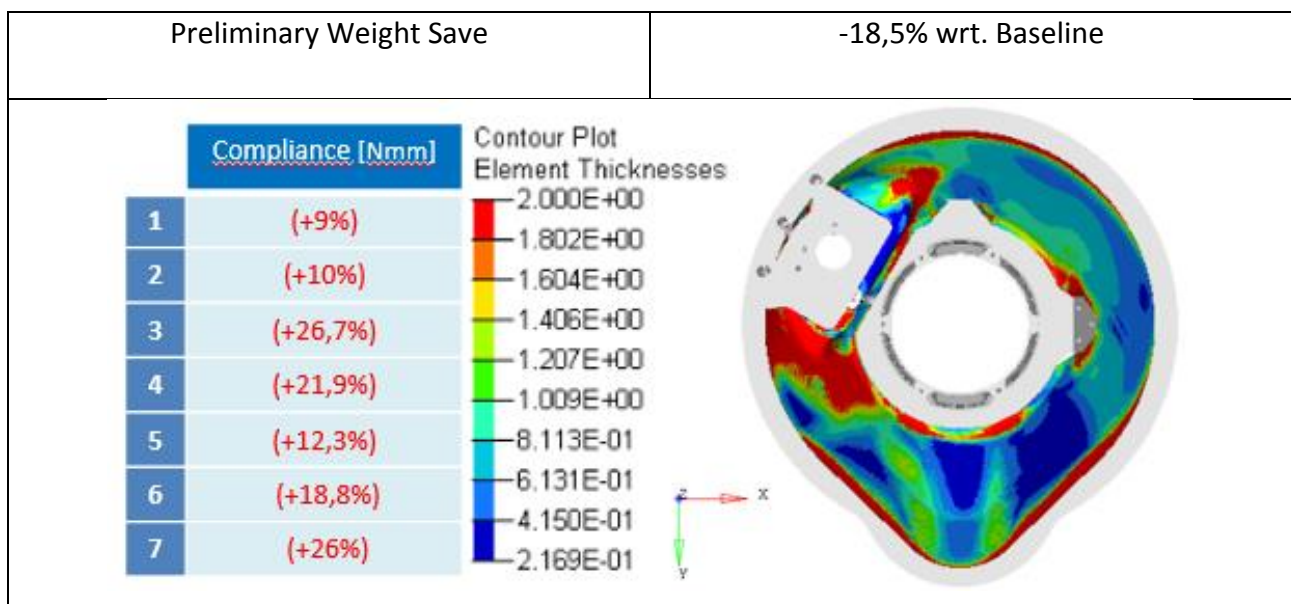


Table 14.1 Weight Save, Compliance and Contour plot of Element Thicknesses with Free-Size optimization on Shell Design

6.3.2 Topography on Shell Design

With Topography optimization nodes as morphed following rules explained in literature. By the fact that this optimization can move nodes, an increase of mass could be expected. For this reason, thickness has been chosen to globally reduce the mass. For stress value same considerations of Free-Size optimization have been done. The settings of Topography optimization are shown in Table 15 and results are presented in Table 15.1. Compliance for each load condition result considerably increased also comparing previous results.

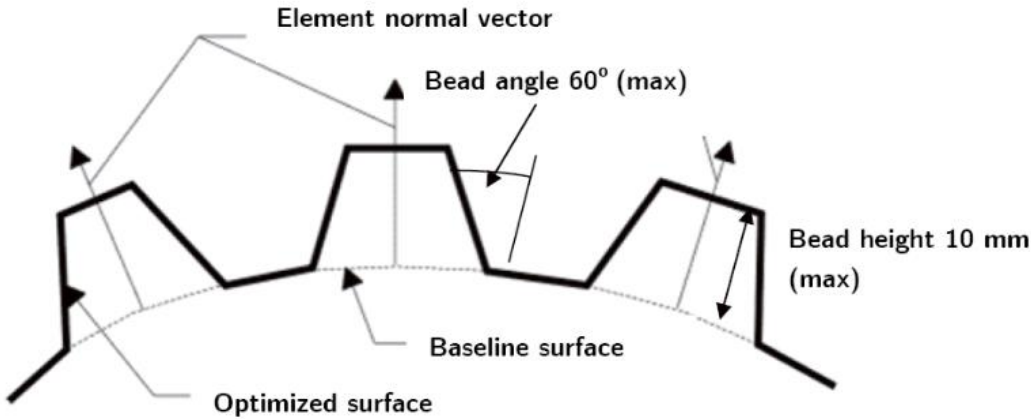
Objective	Minimize Mass
Optimization Constraints	PCU displacements (baseline) BALL displacements (baseline) ROLL displacements (baseline) Stress (55 % of UTS)
Optimization Parameters	Minimum Width = 8 [mm] Draw Angle = 60 [°] Draw height = 10 [mm]
	

Table 15 Topography optimization on Shell Design and bead parameters

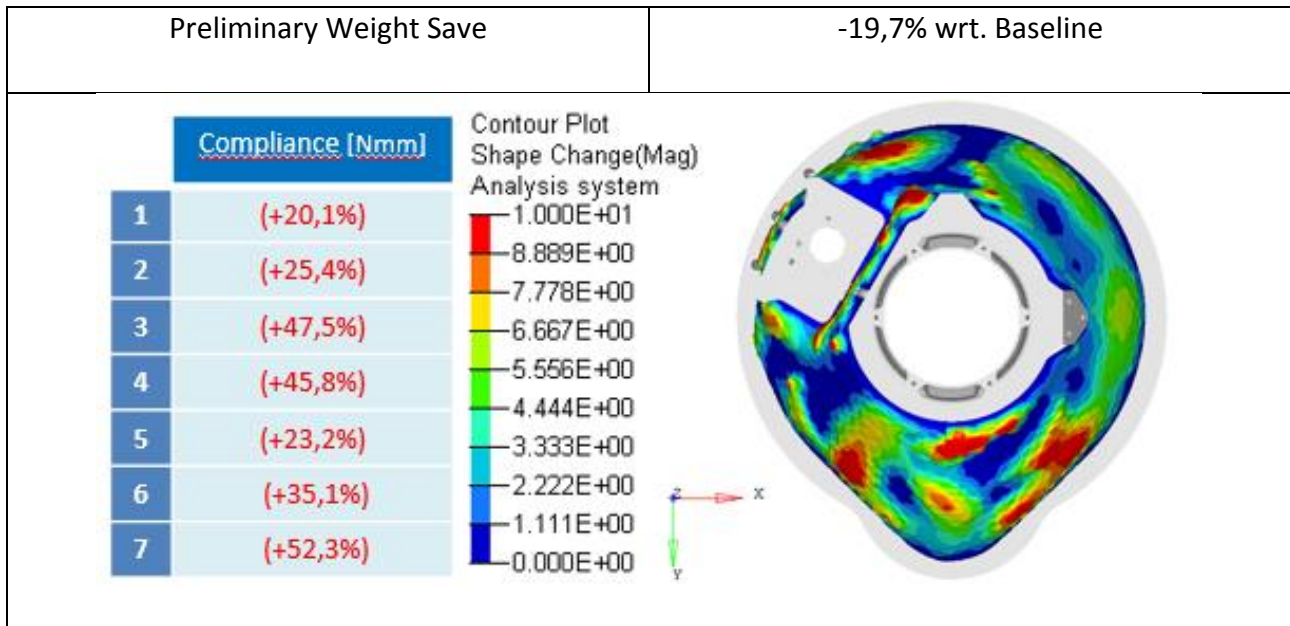


Table 15.1 Weight Save, Compliance and Contour plot of Shape Change with Topography optimization on Shell Design

6.3.3 Topology on Design Space 3D

From literature is clear that Topology optimization is widely used, especially for design components with AM processes. Topology optimization is usually used to identify load path of structures. Being a Concept Design to not strictly constraint the responses is advised. For this reason, for this optimization, increased displacements of 15% comparing to the baseline have been chosen.

A lot of optimizations have been done to identify the best parameters combination. Design space has been changed during the work to assist solver and to properly consider tubes. The last set of parameters and Design Space are now reported.

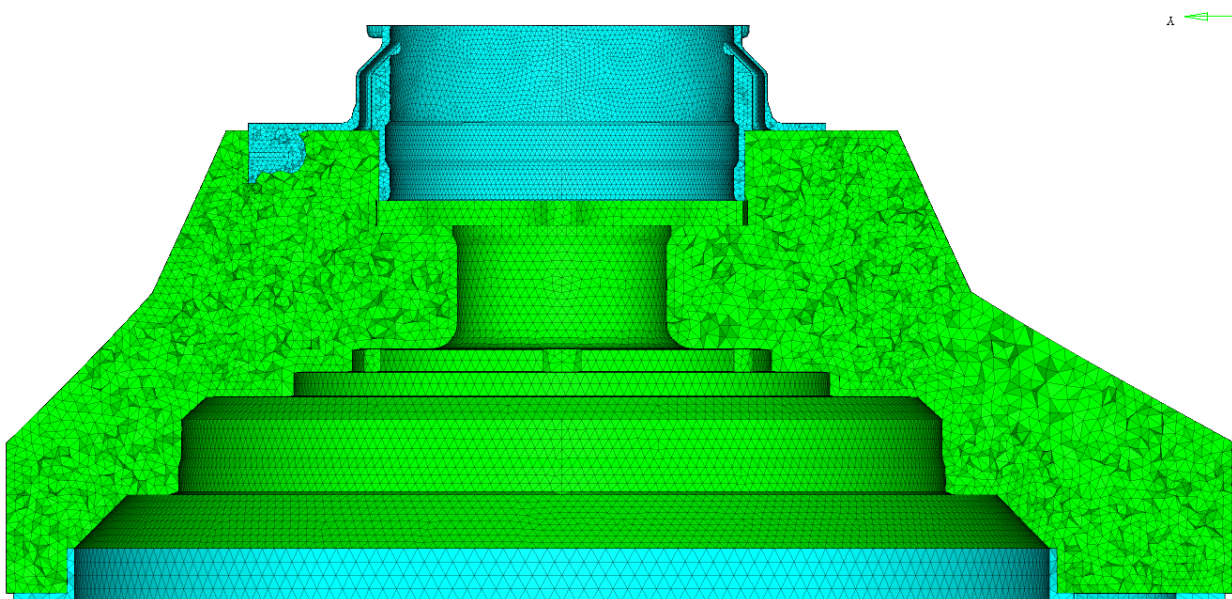


Figure 47 Section of Design Space 3D

Objective	Minimize Mass
Optimization Constraints	PCU displacements (+15% wrt. baseline) BALL displacements (+15% wrt. baseline) ROLL displacements (+15% wrt. baseline)
Optimization Parameters	MINDIM = 30 mm DISCRETE = 3 MMCHECK = 1

Table 16 Topology optimization on Design 3D

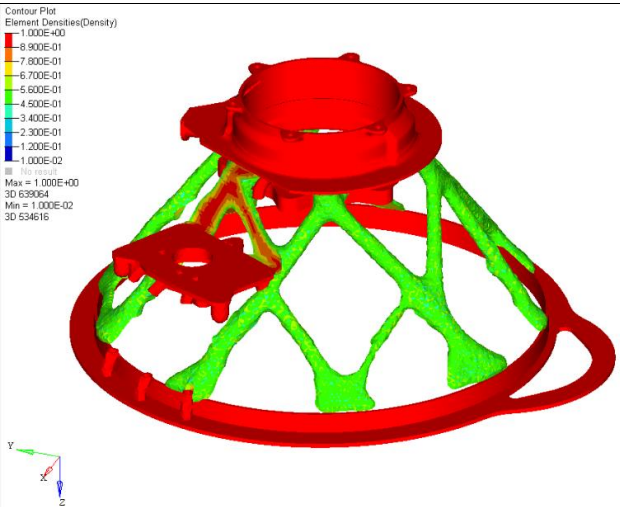
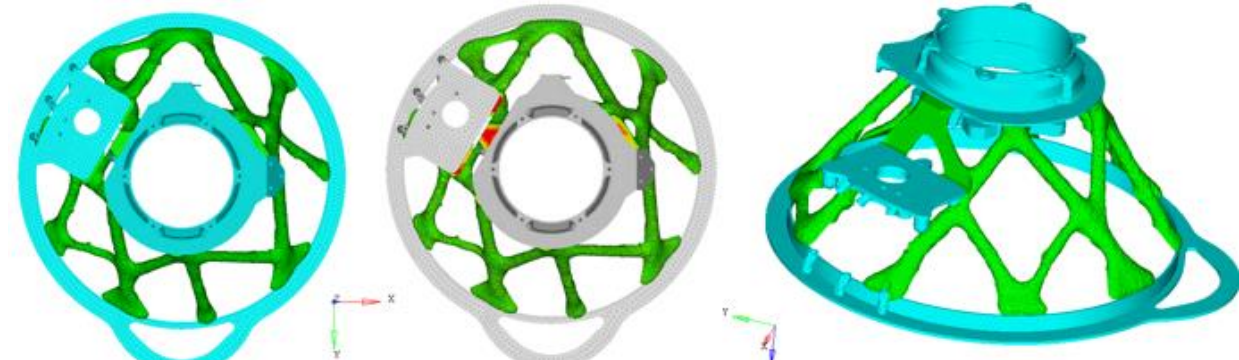
Preliminary Weight Save	-19,0% wrt. Baseline																
<table border="1"> <thead> <tr> <th></th><th>Compliance [Nmm]</th></tr> </thead> <tbody> <tr> <td>1</td><td>(+20,1%)</td></tr> <tr> <td>2</td><td>(+14,9%)</td></tr> <tr> <td>3</td><td>(+52,9%)</td></tr> <tr> <td>4</td><td>(+46,8%)</td></tr> <tr> <td>5</td><td>(+22,3%)</td></tr> <tr> <td>6</td><td>(+41,7%)</td></tr> <tr> <td>7</td><td>(+43,1%)</td></tr> </tbody> </table>		Compliance [Nmm]	1	(+20,1%)	2	(+14,9%)	3	(+52,9%)	4	(+46,8%)	5	(+22,3%)	6	(+41,7%)	7	(+43,1%)	
	Compliance [Nmm]																
1	(+20,1%)																
2	(+14,9%)																
3	(+52,9%)																
4	(+46,8%)																
5	(+22,3%)																
6	(+41,7%)																
7	(+43,1%)																
																	

Table 16.1 Weight Save, Compliance and Elements densities (threshold value of 0,5) with Topology optimization on Design 3D

6.3.4 Conclusion of Conceptual Design

Keeping in mind steps of 3.2, Design and Non-Design Space are defined at the beginning of 6.2 and responses are defined case-by-case in each analysed optimization (step 1). By three Conceptual Design optimizations analysed, Topography optimization results most promising in terms of mass and Free-Size result the best solution in terms of compliance. But considering difficulties to produce with AM geometries with variational section along grow direction and at the same time the necessity to maintain an overhang limit angle of 45° (Topography), and to make matters worse, considering the overmentioned problem of limit stress values for a thin wall (Topography and Free-Size), optimization solutions applied on Shell Design Space have been currently not taken into account. Furthermore, is known by literature the opportunities that Topology optimization offer to produce a component with AM (step 2). For these reasons in conclusion of step 2 described in 3.2, exploration of Conceptual Design optimization could be considered concluded choosing Topology optimization as the most promising (step 3). Results of Topology optimization are re-analysed and verified showing consistency with Topology results (step 4). Notice that this re-analysis should be done on reconstructed geometry, but knowing the difficulties to do this, the verified geometry has been developed without accuracy (mesh 3D starting from .stl file given by results of Topology optimization). For these reasons was impossible switch directly to step 5.

An approximate geometry successively has been done using SoldiThinking Inspire CAD with polynurbs function as shown in fig. 49.

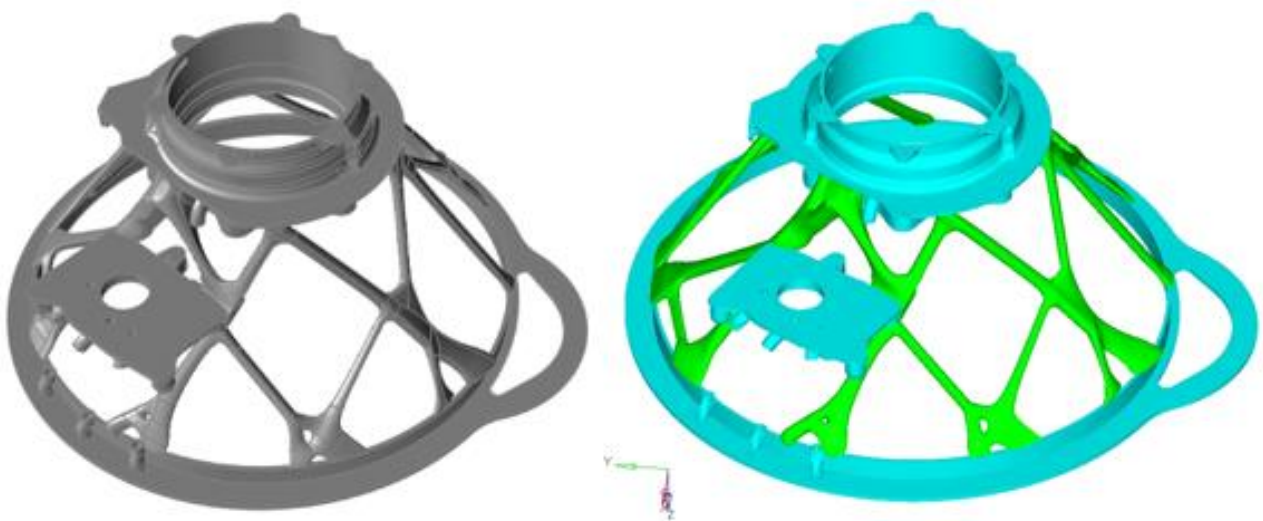


Figure 49 Left: Geometry reconstruction in SoldiThinking Inspire CAD; Right: Mesh of new geometry

Unfortunately, meshing this new geometry, preliminary weight saving results of 10,0% instead of 19,0% (of topology results) comparing these percentage with the baseline. Keeping in mind the aim of the thesis, it has been chosen to continue with steps of guideline instead of spending a lot of time with reconstruction of the geometry. Therefore, at this point we can say to be at step 6 because we have an unacceptable value of mass. To get close to the mass reduction obtained with Topology optimization (19,0%), a Free-Shape optimization has been set as shown in Table 17. Thus, nodes on surface of the new geometry are considered as design variable. Furthermore, constrained displacements are reduced of 15% because of were increased of the same value in Topology optimization. In this way the displacements come back to the baseline values.

Objective	Minimize Mass
Optimization Constraints	PCU displacements (baseline)
	BALL displacements (baseline)
	ROLL displacements (baseline)

Table 17 Free-Shape optimization on new geometry

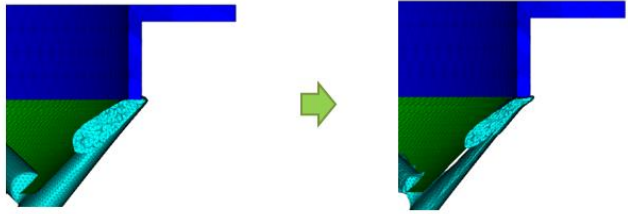
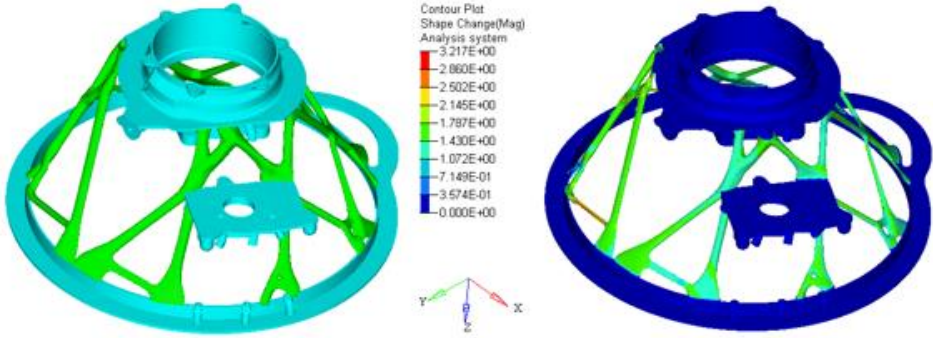
Preliminary Weight Save	-21,9% wrt. Baseline																
<table border="1"> <thead> <tr> <th></th><th>Compliance [Nmm]</th></tr> </thead> <tbody> <tr><td>1</td><td>(+10,9%)</td></tr> <tr><td>2</td><td>(+7,4%)</td></tr> <tr><td>3</td><td>(+42,9%)</td></tr> <tr><td>4</td><td>(+35,7%)</td></tr> <tr><td>5</td><td>(+14,5%)</td></tr> <tr><td>6</td><td>(+34,7%)</td></tr> <tr><td>7</td><td>(+30,2%)</td></tr> </tbody> </table>		Compliance [Nmm]	1	(+10,9%)	2	(+7,4%)	3	(+42,9%)	4	(+35,7%)	5	(+14,5%)	6	(+34,7%)	7	(+30,2%)	
	Compliance [Nmm]																
1	(+10,9%)																
2	(+7,4%)																
3	(+42,9%)																
4	(+35,7%)																
5	(+14,5%)																
6	(+34,7%)																
7	(+30,2%)																
																	

Table 17.1 Weight Save, Compliance and Shape change as result of Free-Shape optimization on new geometry;
Left: mesh on new geometry; Right: result of Free-Shape optimization

Values of displacements and values of stresses are checked and shown according with step 4 in fig. 51:

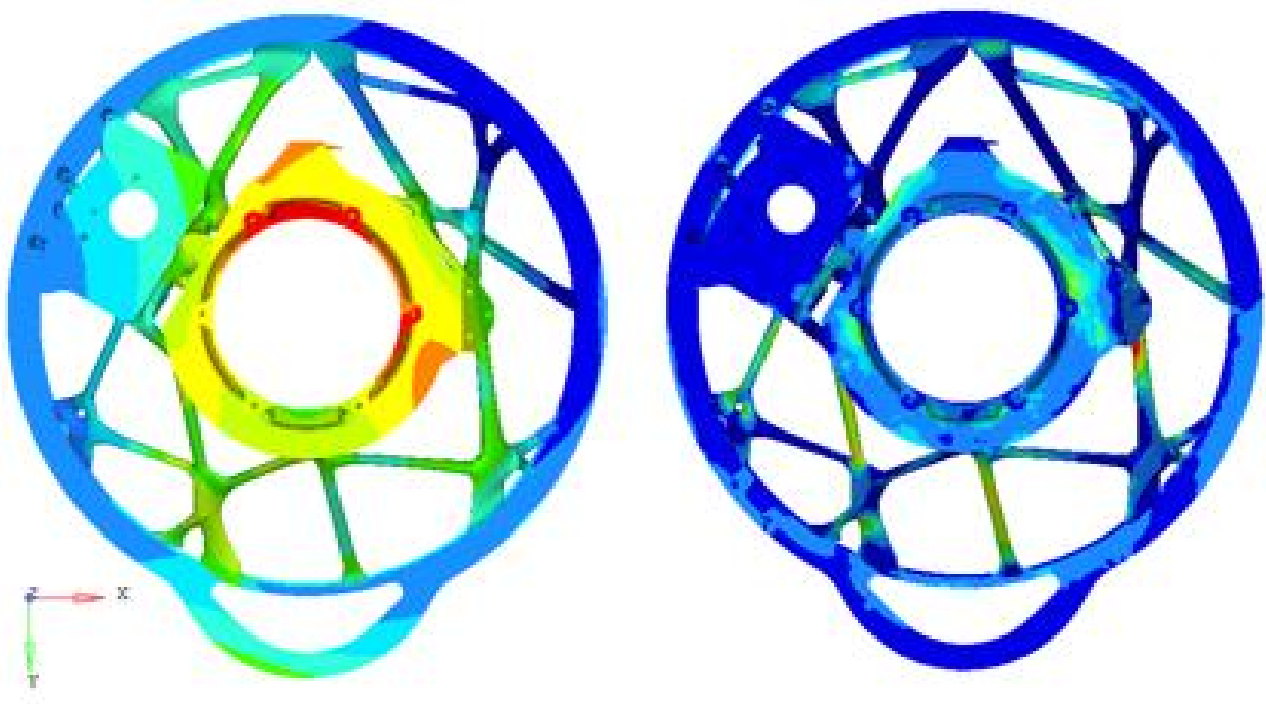


Figure 51 Re-analysis on Free-Shape optimization results

With Free-Shape optimization (Define Fine-Tuning) is shown how it is fast and useful to reach results that are satisfactory starting from a well-defined problem of Conceptual design. Looking at results there are some zones that need to be optimized to reduce the local stress value. For the sake of simplicity also these parts are considered optimized.

Moreover, this component need to be covered adding a panel that could be a disadvantage in terms of mass but an advantage in terms of stiffness of the structure (compliance).

Shell surface that can cover load path has been developed in a way to spend less material as possible but considering manufacturing constraint. The major issue is represented by zone that cover drain. In first approximation was decided to connect drain zone with upper part keeping 45 ° between wall and Z axis. Furthermore, minimum thickness of 0,2 [mm] is considered according to manufacturing constraint. With panel, the reduction of mass is 18,0% instead of 21,9%. The complete proposal is shown in fig. 52 and considering results as satisfactory now it is possible to start the Design Validation process.

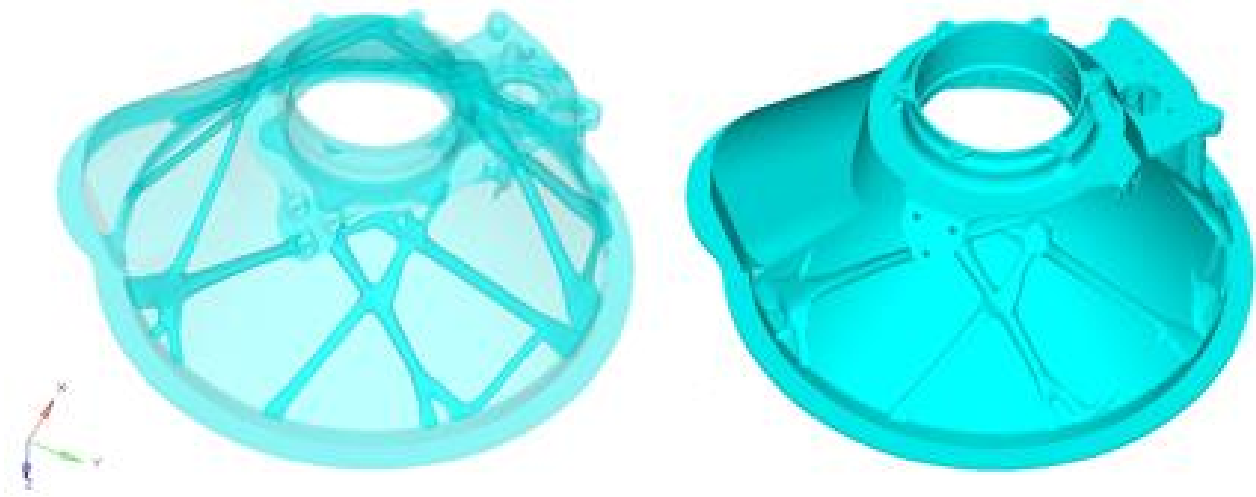


Figure 52 Final design proposal

6.3 Design Validation

Before to move to the Design Validation phase some considerations about productivity for AM have been done. A best practise for AM is to maintain as much as possible constant section of melted material to reduce issues related to the technology (thermal stresses and roughness). Fortunately, geometry obtained by Topology optimization maintain its arms with section almost constant. The geometry is covered by a panel and at the intersection of this with load path obtained by optimization, there is a significant difference of section and likely the design need an adjustment. The thickness of the panel will be increased deeming a post machining operation to obtain a best superficial roughness to limit crack propagation due to fatigue loads. Choosing vertical grow direction middle flange marks a criticality. Printing from top flange to the bottom one certainly there is necessity to introduce supports resulting middle flange an overhang feature at 90°. Instead, printing in opposite direction middle flange could be self-supported by surrounding material. Choosing this second grow direction, the bottom flange need to be careful constrained to the plate of 3D printing machine to avoid separation of the layers due its relatively large size. After the design have been deemed to be printable, the task of finalizing the design need to be undertaken.

Moving to the Design Validation phase component will be submitted to various analyses as ultimate test, LCF, HCF etc. When the design showed that it would meet all specifications, the corresponding STL file need to be imported into suitable software to prepare for printing describing orientation of the part on the build platform and by providing required supports [13].

Conclusions

In this thesis work a strong guideline has been developed to design or re-design structural components. It has been discussed the discretization depending on geometry of object of study and different responses. It has been useful to choose the right kind of optimization available. Some efforts have been done to consider dynamic behaviour and manufacturing constraint of overhang during optimization process. A good practice before to optimize real component is to build a dummy similar case in a way to understand main issues of the analysed problem.

With real test case has been shown that Design Optimization could be characterized by more optimization loop. It means that not just one kind of optimization has to be explored. As instance Topology optimization results useful to define load path but without severe constraint. For this reason, other optimization, like Free-Shape, could be done on geometry that result by Topology optimization in order to reach desired behaviour (stress; compliance; displacement; mass). Some considerations useful for AM process during optimization phase have been done.

Nevertheless it is important to remark that other kind of optimizations could be done; to set combined optimization on load path obtained by Topology optimization (Free-Shape, Shape, Topography, Topology, Lattice) and on thin wall added to cover the part (Free-Size, Topography); Lattice optimization on Design 3D; lattice optimization on reconstructed geometry; to cover load path obtained by Topology optimization and run a Size or Free-Size optimization; to cover load path obtained by Topology optimization with a thin layer of material and fill it with lattice structure.

From chapter 6.3 is clear that is not possible reach directly the Design Validation phase due to impossibilities to consider all adjustment for AM during optimization phase with actual instrument. Indeed, there is a necessity to begin a loop process to reach pre-established objective with particularities of AM. After, it is possible to go ahead with Design Validation process and if some specification is not satisfied, there is a necessity to modify again the geometry.

In the future could be interesting compacting Design Optimization phase with as regard AM process of Design Validation to avoiding unnecessary loop optimization phases saving time. As instance much efforts can be spent in research to introduce residual thermal stress in the simulation.

Bibliography

- [1] Mikko Hovilehto, Lauri Jokinen, Pasi Holopainen, Antti Salminen, Heidi Piili, 9th International Conference on Photonic Technologies LANE 2016, *Design of a hydraulic component for additive manufacturing of stainless steel*.
- [2] Chee Kai Chua, Kah Fai Leong, *3D Printing and Additive Manufacturing*.
- [3] Journal of Laser Applications 24, 050101 (2012); doi: 10.2351/1.4745081.
- [4] Albert E. Patterson, Sherri L. Messimer, Phillip A. Farrington (2017). *Overhanging Features and the SLM/DMLS Residual Stresses Problem: Review and Future Research Need*.
- [5] Peter Mercelis and Jean-Pierre Kruth, Division PMA, Department of Mechanical Engineering, University of Leuven, Leuven, Belgium, *Residual stresses in selective laser sintering and selective laser melting*.
- [6] Sundar, R.; Hedao, P.; Ranganathan, K.; Bindra, K.S.; Oak, S.M (2014). Application of Meshes to Extract the Fabricated Objects in Selective Laser Melting. *Mater. Manuf. Process*.
- [7] Tutorial Netfabb (2018). <https://www.youtube.com/watch?v=1zXQh6Wfpos>.
- [8] Daniel Thomas, Ph.D. Thesis, University of Wales Institute, Cardiff (2009). *The Development of Design Rules for Selective Laser Melting*.
- [9] Altair University, Academic Program, Practical aspects of Structural Optimization, a Study Guide.
- [10] HyperWorks, OptiStruct User's Guide and Tutorials.
- [11] Cavazzuti M., MilleChili Lab, DIMeC, Università degli Studi di Modena e Reggio Emilia (2013). *Introduzione alle tecniche di ottimizzazione*.
- [12] Altair HyperWorks, <https://altairhyperworks.com/solution/Optimization>.
- [13] Erin Komi, research report VTT-R-03159-16. *Design for additive manufacturing*.
- [14] Salmi A., Department of Management and Production Engineering, Politecnico di Torino (2017). *Design Guidelines for Direct Metal Laser Sintering (DMLS)*.
- [15] Sreeram Polavarapu, Clemson University (2008). *Topology and free-size optimization with multiple loading conditions for light weight design of die cast automotive backrest frame*.
- [16] Jiaqin Chen, Vadim Shapiro, Krishnan Suresh, Igor Tsukanov. *Parametric and topological control in shape optimization*.
- [17] G. Allaire, C. Dapogny, R. Estevez, A. Faure, and G. Michailidis. *Structural optimization under overhang constraints imposed by additive manufacturing technologies*.
- [18] Bendsoe M.P., Sigmund O. (2003). *Topology Optimization Theory, Methods and Application, Second Edition, Springer*.

- [19] T. Gao, W. Zhang, P. Duysinx. *Comparison of volume constraint and mass constraint in structural topology optimization with multiphase materials*.
- [20] Rojas Labanda, Susana; Stolpe, Mathias; Sigmund, Ole (2015). *Mathematical programming methods for large-scale topology optimization problems*.
- [21] A. Gugliotta, Politecnico di Torino, Dipartimento di Meccanica (2002). *Elementi finiti*.
- [22] Graeme J. Kennedy, School of Aerospace Engineering, Georgia Institute of Technology, Atlanta, Georgia. *Large-Scale Multimaterial Topology Optimization for Additive Manufacturing*.
- [23] D. W. Adams, C. J. Turner¹ Department of Mechanical Engineering, Clemson University, Clemson, SC 29631. *Implicit slicing method for additive manufacturing processes*.
- [24] Yu-an Jin & Yong He & Jian-zhong Fu. *Support generation for additive manufacturing based on sliced data*.
- [25] A. Jansson O. Edholm, Stockholm, Sverige (2016). *Scale factor and shrinkage in additive manufacturing using binder jetting*.
- [26] Laurent Van Belle, Jean-Claude Boyer, Guillaume Vansteenkiste. *Investigation of residual stresses induced during the selective laser melting process*.
- [27] Qingbo Jia, Dongdong Gu. *Selective laser melting additive manufacturing of Inconel 718 superalloy parts: Densification, microstructure and properties*.
- [28] Lawrence E. Murr, Edwin Martinez, Krista N. Amato, Sara M. Gaytan, Jennifer Hernandez, Diana A. Ramirez, Patrick W. Shindo, Frank Medina, Ryan B. Wicker. *Fabrication of Metal and Alloy Components by Additive Manufacturing: Examples of 3D Materials Science*.
- [29] Raffaele Di Maro, Politecnico di Torino (2017). *Topology optimization of aircraft components for additive manufacturing*.
- [30] Avio Aero a-GE business, Who we are. <http://www.avioaero.com/eng/Who/Avio-Aero>.
- [31] Avio Aero, Piedmont witnesses the birth of 3D printing for the aeronautics industry of the future (2013) .<https://www.avioaero.com/eng/Press-releases/AVIO-AERO-Piedmont-witnesses-the-birth-of-3D-printing-for-the-aeronautics-industry-of-the-future>.
- [32] About Magazine website, Laser machines in the University (2017). <https://www.magazineabout.com/eng/Sites/About-Magazine/Research-Education/Laser-machines-in-the-University>.
- [33] GE Reports, GE's 3D-Printed Airplane Engine Will Run This Year (2017). <https://www.ge.com/reports/mad-props-3d-printed-airplane-engine-will-run-year>.

- [34] GE Aviation, GE Aviation announces first run of the Advanced Turboprop engine (2017). <https://www.geaviation.com/press-release/business-general-aviation/ge-aviation-announces-first-run-advanced-turboprop-engine>.
- [35] Carmelo Giorgio, Politecnico di Torino (2016-2017). *Dinamica di sistema per un motore turboelica di nuova generazione*.
- [36] MIL-HDBK-17-3E, Working Draft, Chapter 6 Structural Reliability.
- [37] Giancarlo Genta, Springer, *Vibration Dynamics and Control*.
- [38] Ola Flodén, Kent Persson, Goran Sandberg, Lund University, Department of Construction Sciences, P.O. Box 118, SE-22100 Lund, Sweden. *Reduction methods for the dynamic analysis of substructure models of lightweight building*.
- [39] Bruno A. Olshausen, PSC 129 – Sensory Processes (2000). *Aliasing*.
- [40] John T. Young. Primer on the craig-bampton method.
- [41] Master of Science Thesis, University of Alabama, Huntsville, AL, USA (2014). Available online: <http://gradworks.umi.com/15/89/1589147.html> (accessed on 11 April 2017). *Patterson, A.E. Design of Experiment to Analyze Effect of Input Parameters on Thermal Stress and Deformation in Overhanging Part Features Created with the SLM Additive Manufacturing Process*.
- [42] How does the Pratt & Whitney Canada PT6 differ from other turboprop engines. <https://aviation.stackexchange.com/questions/22151/how-does-the-pratt-whitney-canada-t6-differ-from-other-turboprop-engines>.